Progress Report on

# Rational Design of FePtK/SiO$_2$ Fischer-Tropsch Catalysts and Study on Their Activity-Nanophase Relationships

By

Jian Xu, and Calvin H. Bartholomew, Professor

BYU Catalysis Lab, Dept. of Chemical Engineering, 350CB

Brigham Young University

Provo, Utah 84602

December 5, 2001

# TABLE OF CONTENTS

# LIST OF TABLES

# LIST OF FIGURES

# I. BACKGROUND AND OBJECTIVES

## Background

The synthesis of hydrocarbons from coal and natural gas (Fischer-Tropsch synthesis) has been known since the late 1920s. In light of decreasing crude oil resources, coal and natural gas are promising feedstock alternatives for the chemical and fuel industries. As oil prices continue to increase, the conversion of natural gas to liquid hydrocarbons via the Fischer-Tropsch synthesis (FTS) becomes economically promising. In addition to SASOL and Shell, who are running commercial FTS plants, other companies including Exxon-Mobil, BP-Amoco, and Chevron-Texaco are actively seeking to develop their own FTS processes, license FTS technologies, and build plants to process natural gas.

Many studies have been and are being carried out to develop or improve commercial technologies for FTS. Among these efforts, catalyst technology development plays a key role. Current FTS catalysts include cobalt, ruthenium and iron promoted with copper, potassium, and other oxides. Iron catalysts are used for FTS because of their remarkable water-gas shift (WGS) activity and low cost. Depending on the desired product and operating pressure and reaction conditions, iron catalysts can be used in a multi-tube fixed bed reactor or slurry bubble-column reactor (SBCR). In the slurry process iron catalysts are suspended in the liquid product to improve mixing and heat removal. Slurry reactor technology provides substantial economic benefits for mainstream FTS.

Unfortunately iron catalysts used in the slurry phase process encounter serious problems. First, iron catalysts undergo serious attrition during reaction, producing micron-sized catalyst particles that increase the viscosity of the slurry phase. These catalyst fine particles can cause fouling of downstream equipment and make the separation of the catalyst from the wax product extremely difficult. The deactivation and attrition of Fe catalysts in SBCR are due to not only physical processes (e.g., vigorous movement and collision of catalyst particles leading to erosion and attrition) but also to chemical factors e.g. phase changes during pretreatment and reaction. Second, iron catalysts deactivate within 2,000-5000 hours of use and are generally not regenerable, this also increases the operating cost.

Although an SBCR offers more advantages than a fixed bed or fluidized bed reactor, it requires an iron catalyst of high attrition-resistance. At present, the most active, selective iron catalysts are unsupported Fe/Cu/K catalysts prepared by precipitation. Precipitated iron catalysts (Fe/Cu/K/$SiO_2$) prepared at Texas A&M University (TAMU) are reported to be more active than precipitated iron catalysts prepared by Mobil and Rheinpreussen [Bukur et al., 1998 and 1999]. Moreover, based on preliminary tests [Pham, 1999], TMAU' s catalyst also has fairly high attrition resistance, although more work is needed to quantify this behavior. Nevertheless, it is conceivable that even the strongest precipitated iron catalysts may not have adequate attrition resistance. Accordingly, there is interest in developing alternative catalysts of high attrition resistance; for example, silica- or alumina-supported iron catalysts. Moreover, addition of noble metal promoters such as Pt to the iron catalyst may improve its reducibility to iron metal and carbides and its regenerability, while enhancing activity maintenance as in cobalt bimetallic FTS catalysts.

### Objectives of Research Program

The principal objectives of this program are to:

1. Prepare active, selective and attrition-resistant silica-supported Fe and Fe-Pt FTS catalysts of high iron reducibility and dispersion.

2. Understand the effects of catalyst preparation, pretreatment, reaction and promoter (Pt) on iron phase transformations.
3. Obtain an understanding of important preparation-activity-structure relationships such as the effects of reduction temperature on activity, dispersion and state of reduction.

**Approach**

To accomplish these objectives, an experimental plan has been designed which incorporates (1) a novel preparation involving non-aqueous (acetone) evaporation deposition of metal salts on a dehydroxylated support to facilitate uniform penetration of support pores, high iron reducibility and high metal dispersion; (2) the application of in-situ Mössbauer and HRTEM to the understanding of Fe chemical speciation and crystallite morphology; (3) temperature programmed reduction (TPR), $H_2$ chemisorption, HRTEM and BET surface area measurements coupled with activity and stability tests of the unpromoted and promoted catalyst in a fixed bed reactor under industrially-relevant process conditions; and (4) a detailed statistical fixed bed experiment design using the L18 orthogonal array in the study of iron FTS catalysts that was formulated with help from the BYU Statistic Consultation Laboratory. Prior to this experimental design, a preliminary study of silica-supported Fe and Fe-Pt bimetallic catalyst was carried out. Both unpromoted and promoted catalysts were tested in a fixed bed reactor at various conditions useful in scoping parameters for the statistical experiment design. Factors in these experiments included catalyst composition, pretreatment gas composition, pretreatment temperature and fixed reaction temperature. The statistically designed experiments should provide a scientific basis for development of an iron FTS catalyst, which is attrition-resistant, highly active and highly stable.

This report summarizes the results of the scoping experiments and data obtained in several statistically designed experiments.

## II. EXPERIMENTAL

### Catalyst Preparation and Compositions

A non-aqueous (acetone) evaporative deposition method was used in the preparation of three catalysts: 10 wt% Fe/$SiO_2$, 10 wt% Fe/1.0 wt% Pt/$SiO_2$ and 10 wt% Fe/1.0 wt% Pt/0.2 wt% K/$SiO_2$. Following are the steps of the preparation procedures:

Preparation of 10 wt% Fe/$SiO_2$:

1. Dried desired amount of Davisil 644 support at 600 °C for 24 h.
2. Dried desired amount of $Fe(NO_3)_3{\cdot}9H_2O$ in flowing air at 100 °C for 24 h to remove waters of hydration.
3. While the dried $Fe(NO_3)_3$ was still hot, 100 ml of acetone was poured into the beaker and stirred until the solid dissolved.
4. Transferred the dried Davisil 644 support into a flask with a top mounted mechanical stirrer. Measured 200 ml of acetone and poured into the flask washing the Davisil 644 on the wall of flask; stirred to form a slurry.
5. Bubbled He gas through the slurry at a rate of 100 SCCM.
6. Poured the 100 ml dried iron nitrate into the slurry.
7. Continued bubbling of He and stirring until the acetone liquid was evaporated.
8. Dried the wet catalyst paste at 80°C for 24 h in a oven, put the dried catalyst (of dark orange color) in a sample vial and stored in a desiccator.

Preparation of 10 wt% Fe/1.0 wt% Pt/$SiO_2$:

1. Dissolved suitable amount of Pt amine salt in 100 ml of acetone to form a solution.
2. Measured the desired amount of dried 20 wt% Fe/$SiO_2$ catalyst and added it to acetone to form a slurry. Transferred the slurry to the same mechanically stirred flask (as above).
3. Bubbled helium gas through the catalyst slurry.
4. Started the mechanical stirrer and slowly introduced the Pt salt solution.
5. Bubbled He and stirred until all acetone liquid was evaporated.
6. Dried the wet catalyst paste at 80 °C in vacuum oven with flowing He for 24 h.
7. Transferred the dried catalyst (of dark orange color) to a vial and stored it in a desiccator.

<u>Preparation of 10 wt% Fe/1.0 wt% Pt/0.2 wt% K/$SiO_2$:</u>

1. Dried desired amount of Davisil 644 support at 600 °C for 24 h.
2. Dried desired amount of $Fe(NO_3)_3 \cdot 9H_2O$ in flowing air at 100 °C for 24 h.
3. While the dried Fe $(NO_3)_3$ was still hot, 100 ml of acetone was poured into the beaker and stirred until the solid dissolved.
4. Transferred the dried Davisil 644 support into a flask with a top mounted mechanical stirrer. Measured 200 ml of acetone and poured into the flask washing the Davisil 644 on the wall of flask; stirred to form a slurry.
5. Bubbled He gas through the slurry.
6. While the slurry was bubbling, weighed the desired amount of $KNO_3$ and dissolved it in about 4 ml water in a small vial to form a solution.
7. Poured the 100 ml dried iron nitrate into the slurry.
8. At the same time, poured the $KNO_3$ solution into the slurry.

9. Continued bubbling of He and stirring until the acetone liquid was evaporated.
10. Dried the wet catalyst paste at 80°C for 24 h, put the dried catalyst (of dark orange color) in a sample vial and stored in a desiccator.
11. Took this K promoted catalyst out from desiccator and calcined it in He at 200°C for 3 h. Weighed desired amount of this catalyst and calculated the weight of Pt salt needed for 1.0 wt% Pt in final catalyst, dissolved suitable amount of Pt amine salt in 100 ml of acetone to form a solution.
12. Transferred the dried Fe/K/$SiO_2$ support into a flask with a top mounted mechanical stirrer. Measured 200 ml of acetone and poured into the flask; stirred to form a slurry.
13. Started the mechanical stirrer and slowly introduced the Pt salt solution.
14. Bubbled He and stirred until all acetone liquid was evaporated.
15. Dried the wet catalyst paste at 80 °C in vacuum oven with flowing He for 24 h.
16. Transferred the dried catalyst (of dark orange color) to a vial and stored it in a desiccator.

### BET Surface Area and Hydrothermal Stability Tests

BET surface areas were obtained using a Gemini 2360 surface area analyzer. Approximately 0.15 g catalyst samples were degassed in He at 200°C for 2-3 h before test. The hydrothermal stability tests were performed in a 1 cm I.D. fixed-bed reactor with a temperature controller. The steam pressure was regulated using a high-pressure water pump. The steam partial pressure was in a range of 0 to 5 atm. Two grams of support (fresh or modified) was used in these tests. Each support was exposed to steam at 265°C for 72 hours. The steam treated catalyst was then removed from the fixed bed reactor and dried at 80°C in oven for 24 hours before BET measurements. For every support, the hydrothermal stability test was repeated once.

## TGA Studies

A Perkin-Elmer TGA7 system was used in temperature-programmed studies of decomposition in Ar (TPAr), oxidation in 10% $O_2$ in Ar (TPO), and reduction in 10% $H_2$ in Ar (TPR) of fresh catalysts and catalysts after fixed bed activity runs. The catalysts were also exposed to a flow of syngas ($CO/H_2=1$) during programmed linear heating to study the effects of syngas pretreatment.

## Mössbauer Spectroscopy

Mössbauer spectra were obtained using an Austin S-600 spectrometer system with a laser absolute velocity calibrator that enables peak positions to be determined to within $\pm$0.01 mm/s [Stoker, 1999]. The gamma ray source was $^{57}$Co in a rhodium matrix. Peak positions and isomer shifts of all spectra are reported with respect to metallic iron. Mössbauer spectra of the unpromoted and promoted catalyst were collected at 77 and 298 K to study iron phase transformations during synthesis in the fixed bed reactor.

Gamma ray counts were obtained as a function of radioactive source velocity and fitted to a series of sextets composed of six Lorentzian lines having equal widths and intensities with the ratios of 3:2:1:1:2:3 using a nonlinear least squares routine described elsewhere [Stoker, 1999]. Peak assignments were based on comparison of the fitted values of Mössbauer spectroscopy parameters with the reported values in the literature.

A 0.3 g sample of passivated catalyst was pressed to a 1-inch diameter wafer. The sample wafer was then placed in a plexiglass cell at 25°C or in an in-situ Mössbauer cell (77°C or in situ runs), which allows in-situ pretreatment in a controlled atmosphere from 77 K to 723 K.

For fresh catalyst and calcined catalysts, Mössbauer spectra were collected at room temperature (298 K). For reaction-aged (in fixed bed) and passivated catalysts, Mössbauer spectra were collected at 77 K and 298 K for each sample. Spectra of catalysts treated *in situ* in 1 atm of syngas ($CO/H_2=1$) were obtained at 298 K.

### Chemisorption

Selective $H_2$ chemisorption uptakes were measured by a flow desorption method using a custom flow system with a thermal conductivity detector (TCD). The details of this system and procedures are described elsewhere [Jones and Bartholomew, 1988]. In this study 1.0 g of iron catalyst was placed in a Pyrex flow cell and was reduced in a mixture of Ar and $H_2$ (40 % $H_2$) at a GHSV of 2000. The sample temperature was increased at 1°C/min to 300°C and held at 300°C for 16 h; it was then cooled with dry ice/acetone to –84°C. At this temperature, the $H_2$ flow was shut off and Ar was introduced to desorb physisorbed $H_2$. The catalyst was then heated quickly to 300°C at 10-20°C/min while the amount of desorbed $H_2$ was measured by TCD.

### Activity Tests

With the help of the BYU Statistics Consultation Lab, fixed bed test runs of FePtK/$SiO_2$ FTS catalysts were designed using an L18 orthogonal array of catalyst composition and pretreatment variables.

#### Design factors

Design factors under investigation in the statistically designed experiments are listed in the following table along with their corresponding factor levels. The fixed bed reaction temperature consists of two levels, while catalyst composition, pretreatment gas and pretreatment temperature each have three levels.

Table 1. Design Factors in Statistically Designed Experiments

| Factors | Number of Factor Levels | Factor Levels |
|---|---|---|
| Catalyst composition | 3 | 10 % Fe/$SiO_2$<br>10 % Fe-1.0 % Pt/$SiO_2$<br>10 % Fe-1.0 % Pt-0.2 K/$SiO_2$ |
| Pretreatment gas composition | 3 | $H_2$/CO=0.1 |
| | | $H_2$/CO=0.5 |
| | | $H_2$/CO=1.0 |
| Pretreatment temperature | 3 | 250°C |
| | | 280°C |
| | | 320°C |
| Fixed bed reaction temperature | 2 | 250°C |
| | | 265°C |

Response Variables

Table 2 lists the dependent variables of interest to this study, the units of measurement and the range of expected values. Study of these variables is expect to enable evaluation and correlation of catalyst preparation variables and physical and chemical properties with catalyst performance (activity, selectivity and stability).

Table 2. Dependent Variables in Statistically Designed Experiments

| Dependent Variable | Units | Range of values |
|---|---|---|
| Conversion, Xco | Vol% | 0-1.0 |
| Selectivity of $C_{5+}$ | Vol% | 40-60 |
| Stability | %/hour | 100 |
| Dispersion | % | 5.0-20.0 |
| BET surface area | $m^2$/g-cat | 0-300 |
| Phase composition | | $Fe_{2.5}C$ (I, II, III), $Fe_3O_4$(SP), $Fe^{2+}$ |
| Morphology | | |

Procedures

Activity tests were carried out in a 1 cm I.D. fixed-bed reactor with a three-zone furnace with a separate controller for each zone. Two grams of catalyst (100-150 mesh) was diluted with 4 g of quartz chips (70 mesh) to minimize the axial temperature gradient. The temperature inside the catalyst bed was measured by a thermocouple inserted into the catalyst bed.

The feed gas was purified using deoxygenation and zeolite traps and metered with calibrated mass flow controllers. The reactor pressure was regulated by an Mighty Mite backpressure regulator. Heavier waxy products were collected in a hot trap while lighter liquid products were collected at ambient pressure in a cold trap at ice temperature. The exit gas was then analyzed for $H_2$, CO, $CO_2$, $CH_4$ and Ar using an HP 5890 gas chromatograph.

The iron catalyst was pretreated in-situ at atmospheric pressure before each activity test. Reactor temperature was increased at 1°C/min to 200°C and held at 200°C for 3 h. A helium flow of 200 sccm was used to decompose the iron nitrates. The temperature was then increased at 0.5°C/min to 290°C and held for 16 h in a mixture of CO and $H_2$ ($CO/H_2=1$) flowing at 200 sccm. The reactor was then pressurized to 150 psi with a gas mixture containing syngas and an argon tracer at a flow of 65 sccm. The reactor temperature was then adjusted to the desired value and the FT reaction was begun.

Calculations of CO conversion and consumption rates and of $CH_4$ and $CO_2$ selectivities were made using the following equations:

(1) CO conversion (fractional conversion):

$$X_{CO} = \frac{(CO/Ar)_{product}}{(CO/Ar)_{feed}}$$

(2) CO conversion rate (mole/$g_{cat}$.s) was calculated by assuming isothermal integral reaction (See details in APPENDIX).

$$-r_{CO} = \eta k P_{CO}^{-0.24} P_{H_2}^{0.74}$$

(3) $CH_4$ selectivity (mole %)

$$S_{CH_4} = \frac{100 \times (CH_4 / Ar)_{product}}{(CO / Ar)_{feed} \times X_{CO} - S_{CO_2} \times X_{CO}}$$

(4) $CO_2$ selectivity (mole %)

$$S_{CO_2} = \frac{100 \times (CO_2 / Ar)_{product}}{(CO / Ar)_{feed} \times X_{co}}$$

## III. RESULTS AND DISCUSSION

### Chemical Analysis of Catalysts

Catalysts prepared in this study and their compositions determined by atomic absorption (AA) are tabulated in Table 3. Most catalysts have a Fe wt% of about 10% with deviation in reasonable range of instrument error. Three catalysts have been used for statistically designed fixed reactor tests: Fe-S-201, FePt-S220 and FePtK-S-218.

### BET Surface Area Measurements and Hydrothermal Stability Tests

The thermal stability of Davisil 644 was tested by heating separate samples in air for 24 h at a temperature ranging from 200°C to 800°C. BET surface area (SA) is plotted against furnace temperature in Fig 1. It is shown that the BET surface area first decreases sharply from 200°C to 400°C, then levels off at 400, 500 and 600°C. After the furnace temperature exceeds 600°C, the surface area starts to drop sharply again. The purpose of heating Davisil 644 support was to dehydroxylate the support; generally a temperature of 600-800°C is needed for substantial removal of hydroxyl groups. Hence a trade-off was to select 600°C as the support heating temperature.

Changes in BET surface area for impregnated iron catalysts after drying, calcination, and fixed bed reaction are shown in Table 4. After drying at 80°C for 24 h, both catalysts (Fe-S-203, FePt-S-203) have BET surface areas of about 240 $m^2$/gcat (244 $m^2$/gcat and 241 $m^2$/gcat respectively). The unpromoted iron catalyst (Fe-S-206) appears to lose two-third of its surface area after a 55 h fixed bed run; i.e., it has a BET surface area of only 67 $m^2$/gcat. The reason for this low surface area may be due in part to the incomplete removal of wax formed during the fixed bed run, which is likely to block the pore structures of this catalyst. Similarly, FePt-S-206 only has a surface area of 45 $m^2$/gcat after 140 h fixed bed run. After fixed bed run and Soxhlet wax extraction at 110°C, the “true” BET surface area of catalysts such as FePtK-S-215 and FePtK-S-216 can be measured, only a slight decrease in surface area are observed with two catalysts having a BET surface area of 236 and 225 $m^2$/gcat respectively.

It is shown in Fig 2 that steam partial pressures for Fe and Co FTS catalysts under high conversion reaction condition are in the range of 0.5 to 3 atm. Fe FTS catalysts operate at significantly lower water partial pressures (0.5-0.8 atm) because of their high WGS activities. The hydrothermal stabilities of silica support and modified silica supports were tested at water partial pressures in a range of 0 to 5 atm (0, 1.0, 2.0 and 5.0 atm). The results of hydrothermal stability tests in a fixed bed reactor are plotted in Fig 3 for three different silica supports (pure Davisil 644 silica, 3 wt% $FeAl_2O_4/SiO_2$ and 20 wt% $CaAl_2O_4/SiO_2$ modified support). Apparently fresh Davisil 644 support is not hydrothermally stable when exposed to steam partial pressures above 1 atm. Addition of iron aluminates or calcium aluminates improves the hydrothermal stability. At a water partial pressure of 5 atm, the calcium alumninate modified support maintains the highest BET surface area, while the iron aluminate modified support has the second largest BET surface area (98 $m^2$/g). Davisil 644 silica only has a BET surface area of 60 $m^2$/g after similar exposure.

The effect of K promoter effect on thermal stability of Davisil 644 is shown in Fig 4 in the form of BET surface area versus K level. BET surface area decreases with increasing K promoter level. The BET surface area of the 0.2 wt% K promoted support is 8.8 % lower than the value of 285 $m^2/g$ for unpromoted silica. However, upon treatment at 800°C for 24 h, the surface area of 3 % K/Silica drops to essentially zero compared to 190 $m^2/g$ for unpromoted silica under the same conditions.

**Thermal Gravimetric Analysis (TGA)**

TGA studies including TPAr (temperature programmed heating in flowing argon), TPR (temperature programmed reduction in $H_2$) and TPO (temperature programmed oxidation in $O_2$) were carried out on dried unpromoted iron catalysts.

The TPAr spectrum of Fe-S-203 is illustrated in Fig 5. The low temperature peak around 50 to 100°C is attributed to loss of water from the supported iron catalyst. Two large overlapping peaks at 200-295°C are assigned to the decomposition of iron nitrates to iron oxides.

The TPR spectrum of Fe-S-207 after 24 h drying at 80°C is shown in Fig 6. Three peaks are observed during reduction. The first peak around 200°C is probably nitrate decomposition. The second peak around 280°C is probably due to reduction of $Fe_2O_3$ to $Fe_3O_4$. The last peak at 370°C could correspond to FeO being reduced to Fe. An estimate of the degree of reduction of >90 % at 500°C can be obtained from this spectrum. It is evident that some species in the unpromoted iron catalyst (Fe-S-207) are difficult to reduce in $H_2$ even at 370-400°C. At less than 370°C, the extent of reduction of is probably less than 75%.

The effects of addition of a noble metal promoter Pt on extent of reduction of iron FTS catalyst are illustrated in Fig 7 and Fig 8. In Fig 7, a dramatic decrease in reduction temperature is observed for FePt/$SiO_2$ catalyst after calcination at 150°C and 200°C for 3 and 6 h respectively. It is evident that more than 90 % of the iron is reduced to the metal at 400-420°C. A similar conclusion can be drawn after comparing the three spectra in Fig 8, where both FePt-S-206 and FePtK-S-209 have lower reduction temperatures and higher extents of reduction relative to unpromoted Fe. This demonstrates that Pt significantly improves the reduction of Fe/$SiO_2$ catalyst prepared by evaporative deposition.

## Chemisorption Tests

$H_2$ chemisorption and dispersion were measured on calcined catalysts and several catalysts after statistically designed experiments and Soxhlet wax extraction (see Table 5). The average $H_2$ uptake of the unpromoted iron catalyst Fe-S-201 (10.7 wt% Fe/$SiO_2$) after calcination at 200°C and reduction in $H_2$ at 300°C for 16 h is 44.5 μmole/gm-catalyst in three repeated measurements; dispersion is 7.7%. After fixed bed reactor (FBR) run #01 and Soxhlet wax extraction, dispersion unexpectedly increases to an average of 10.4%. This small but significant increase could be due to formation of small crystallites of iron carbide. This phenomenon is not observed, however, for the same catalyst after FBR run #08. Its dispersions are essentially the same as those for calcined Fe-S-201 before reaction with an average of 6.9%. For calcined FePt-S-220 and FePtK-S-218, a trend of increases both in $H_2$ uptake and dispersion after reaction were observed. The average $H_2$ uptake for FePt-S-220 is 51.1 μmol/gcat, while for FePtK-S-218 is 56.5 μmol/gcat. Dispersions of promoted catalysts are based on an assumption that 80% Fe and 100%Pt is reduced; these assumptions are in turn based on TPR (in $H_2$) data. The standard deviation of the uptakes for these two catalysts after statistically designed fixed bed runs were observed to increase, and unexpected increases in $H_2$ uptakes and dispersions were observed. The larger deviation could be due to incomplete wax removal from the pores of these catalysts. But after the surface was cleaned by a few reductions, the apparent dispersions of these two catalysts after FBR runs are significantly lower. For FePt-S-220 after FBR run #09, 4.9%, while for FePtK-S-218 after FBR run #07, the dispersions in third and fourth measurements were 5.1%, and 6.6% respectively.

**Mössbauer Spectroscopy**

A series of spectra collected after fixed bed runs is shown in Fig 9, 10 and 11. Corresponding Mössbauer parameters are listed in Table 6 and Table 7. The spectral areas of iron species of these spectra are summarized in Table 8. The spectral area of $Fe_{2.5}C$ in unpromoted catalyst Fe-S-206 is only 25.6%, compared to 49.3% (298 K) and 51.5% (77 K) for Pt promoted catalyst FePt-S-203. Thus, the Pt promoter significantly enhances formation of $Fe_{2.5}C$ as well as activity in fixed bed runs, suggesting that activity correlates with carbide content. The slightly higher spectral area for $Fe_{2.5}C$ and significantly lower area in small superparamagnetic $Fe_3O_4$ crystallites at liquid $N_2$ temperature indicates that fractions of superparamagnetic $Fe_{2.5}C$ and $Fe_3O_4$ have become ferromagnetic at liquid $N_2$ temperature.

Effects of pretreatment on iron phase transformations were studied in an *in situ* temperature-controlled reactor cell containing a 1-inch 0.3 g catalyst wafer of Fe-S-207. The Mössbauer spectrum collected at room temperature after *in situ* treatment with $H_2$/CO=1 is shown in Fig. 12; corresponding Mössbauer parameters are listed in Table 9. It is evident that iron phases were reduced during the 16 h pretreatment at 280°C in syngas ($H_2$/CO=1), i.e., $Fe_2O_3$ was converted to a mixture of ferromagnetic $Fe_3O_4$ (10.3%), superparamagnetic $Fe_3O_4$ (68.2%), $Fe^{2+}$ (7.5%) and $\chi$-$Fe_{2.5}C$ (14.0%). The peak of low intensity at about 0.89 mm/s (Fig 12) has an isomer shift and quadruple splitting parameters matching these (Table 9) of

$Fe^{2+}$. Thus, for this unpromoted catalyst subjected to 16 h pretreatment in the Mössbauer cell at 280°C and 1 atm, only 14 % $\chi$-$Fe_{2.5}C$ was formed. This lower than expected extent of reduction is to some degree a result of the abbreviated time and low pressure of treatment and in part an artifact of the cell design, i.e. gas flow around but not through the sample. We have redesigned the cell with the introduction of two hollow rings with holes directing gas towards the sample on both sides of the catalyst wafer and a provision for high-pressure treatment. With this improved Mössbauer cell, a series of *in-situ* pretreatment studies will be carried out.

Mössbauer spectra of three catalysts (Fe-S-210, FePt-S-220 and FePtK-S-218) collected at 25°C after 150 h statistically designed FBR runs are shown in Figs 13-21; corresponding Mössbauer parameters are listed in Table 10-18. The spectra areas of different iron phases are summarized in Table 19. A significant fraction (about 50%) is present as magnetite ($Fe_3O_4$) in all catalysts after reaction; However, the amount of $Fe_{2.5}C$ is significantly different for different catalysts. For example, after 150 h FBR run #01 Fe-S-201 only contains 17.5% Hagg carbide, while Pt promoted FePtK-S-218 is observed to contain 44.2% $Fe_{2.5}C$ after run #7. This difference is due in part to promoter effects as well as test run conditions, e.g. pretreatment and reaction temperatures.

Syngas conversion (CO conversion) and iron carbide content ($Fe_{2.5}C$) are plotted in Fig 22 for all catalysts after the statistically designed FBR runs. A fairly strong correlation is observed between iron carbide content and FT activity for catalysts after 150 h FBR reaction except run #08. This observation agrees with the consensus that Hagg carbide ($Fe_{2.5}C$) is the active phase. For example, Fe-S-201 at the end of run #1 has the lowest activity (CO conversion 11%), corresponding to lowest iron carbide content of 17.5% in spectra area. The loss of active phase surface area due to carbon deposition or graphitic carbon formation could also lead to deactivation, especially on the surface layer of the active iron carbide. A detailed statistical analysis will be done after all runs are finished.

## Activity Tests

### *Catalyst Activity and Stability*

Measurements of catalyst activities in terms of CO conversion were carried out in preliminary and statistically designed FBR runs. The purpose of these preliminary runs was to test the effects of Pt promoter and the repeatability of the fixed bed runs and to have preliminary information about the effects of pretreatment. Following these runs, 23, 150 h statistically designed experiments were carried out on three catalysts (Fe-S-210, FePt-S-220 and FePtK-S-218).

The effects of Pt and K promoters on activity are shown by comparison for FePtK-S-215 and Fe-S-201 in Fig 23. Compared to the unpromoted catalyst which reaches a maximum CO conversion of about 84%, the Pt and K promoted catalyst achieves a CO conversion of 97%. But CO conversions for both catalysts level off at about 80% after 130 h FBR run. A remarkable repeatability was observed in Fig 24 for FePtK-S-215 and FePtK-S-216 (two separate batches). Both catalysts reached a maximum conversion of 97% at about the same time and underwent a similar decline in activity during 140 h FBR runs.

The effects of pretreatment on promoted catalysts are shown in Fig 25. Three different pretreatment atmospheres were used: syngas ($H_2/CO = 1.0$), pure $H_2$ and pure CO. The activity of the catalyst pretreated in syngas was initially low but increased to a maximum of 97%, after which its activity declined significantly. On the contrary, the activity of the catalyst pretreated in $H_2$ was initially about 80%, then rapidly declined and stabilized at a conversion of about 70% after which little deactivation was observed. The CO conversion of the catalyst pretreated in CO increased very gradually to about 70% within 200 h; moreover the activity was apparently still unvarying after 200 h. Further studies using *in-situ* Mössbauer spectroscopy and HRTEM are needed to understand these pretreatments effects at the nanoscale.

Before carrying out the statistically designed experiments, the effect of drying the catalyst before reaction was also studied. The result shown in Fig 26 clearly points to a higher activity for catalysts dried before activity testing. Based on these results we conclude that all catalysts should be stored in a desiccator and dried before FBR tests.

Steady-state activities and selectivities for selected unpromoted and promoted catalysts are summarized in Table 20. The promotional effect of Pt (0.5 wt%) may explain the higher activity of FePt-S-206. However, because FePt-S-203 was run at 265°C (lower than 270°C for the unpromoted iron catalyst fixed bed run), the conversion activity is not a great deal higher that that of unpromoted catalyst (Fe-S-206). While the promotional effect of Pt in iron FT catalysts still needs further study, the higher activity of Pt is likely due to improved reduction of iron oxide to active carbide. The higher activity stability may be due to the ability of noble metal to decompose coke precursors [Iglesia et al., 1993; Huber and Bartholomew, 2000] and prevent oxidation of the carbides.

### ***$CH_4$ and $CO_2$ Selectivities***

Methane and $CO_2$ selectivities are also tabulated in Table 20. $CH_4$ selectivities of Pt promoted catalysts are higher than for unpromoted catalysts (9.5% and 10.5% compared to 2.6%). $CO_2$ selectivity for FePt-S-203 is lower than Fe-S-206 (33.3% vs. 36.2), while for

FePt-S-206, $CO_2$ selectivity is higher than that of unpromoted catalyst (38.1% vs. 36.2%). The higher $CH_4$ selectivity for Pt promoted Fe catalyst may be due to a higher hydrogenation activity, which is important in maintaining a clean metal surface and thus preventing fast deactivation. In terms of $CO_2$ selectivities, the catalyst with 0.5 wt% Pt has the lowest value of about 33% from 20 h to 60 h of run time, while the value for unpromoted and 1 wt% Pt promoted catalyst are 35% and 38% respectively.

## IV. CONCLUSIONS

A rationally designed high activity FePtK catalyst supported on attrition-resistant silica was prepared using a non-aqueous (acetone) evaporative deposition technique. Preliminary study of pretreatment, drying effects on catalyst performance and repeatability has been done. 14 statistically designed FBR runs have been finished, room temperature Mössbauer spectra have been collected on 11 samples after run. Conclusions from the present work include the following:

1. Silica support collapse only happens at above 1 atm water partial pressure, with $FeAl_2O_4$ and $CaAl_2O_4$ coated silica support showing improved hydrothermal stability.
2. TPR results show an extent of reduction of 75% is achieved for $Fe/SiO_2$ at less than 370°C. For Pt promoted catalysts, a marked decrease in reduction temperature is observed and 90% reduction of iron metal is possible at 400°C.
3. Using *in situ* Mössbauer analysis, the following iron phase transformations are observed after a 16 h pretreatment at 280°C in syngas ($H_2$/CO=1) at 1 atm: $Fe_2O_3$ is converted to a mixture of ferromagnetic $Fe_3O_4$ (10.29%), superparamagnetic $Fe_3O_4$ (68.24%), $Fe^{2+}$ (7.49%) and $\chi$-$Fe_{2.5}C$ (14%). The lower than expected extent of reduction is possibly due

to the abbreviated time and low pressures of treatment and in part an artifact of the cell design leading to poor gas/solid contact.

4. The Pt promoter significantly improves the dispersion of iron particles on the silica support during reduction in $H_2$ at 300°C. During the FBR runs, dispersions of all catalysts decrease significantly.
5. After reacting for about 60 hours at 265°C and 10 atm followed by passivation, Pt-promoted iron (0.5 wt% Pt) contains a greater percentage of $\chi$-$Fe_{2.5}C$ and a smaller percentage of superparamagnetic $Fe_3O_4$ relative to the unpromoted iron catalyst. Thus, Pt substantially enhances reduction of iron oxides to $\chi$-$Fe_{2.5}C$ while significantly reducing iron-silica support interactions. FePt-S-206 (containing 1% Pt) after testing at 265°C and 10 atm for a total of 140 h and careful passivation contains more superparamagnetic $Fe_3O_4$ (59.9% vs. 48.6%) and less $Fe_{2.5}C$ (40.2 vs. 51.5%) than that of FePt-S-203 (0.5 wt % Pt, 60 h fixed bed run). This difference in phases distribution may be explained by the longer FTS reaction time for the 1 wt% Pt promoted iron catalyst in which more iron carbides are probably converted to superparamagnetic $Fe_3O_4$ during exposure to an oxidizing environment of product steam and $CO_2$. No $Fe^{2+}$ is observed too, which confirms that Pt promotes iron oxides reduction and inhibits the iron-silica support interaction.
6. The activity of Pt-promoted iron is higher than unpromoted iron. This higher activity of Pt is probably due to improved reduction of iron oxide to active carbide. The higher activity stability may be due to the ability of noble metal to decompose coke precursors and moderate oxidation of the carbides.

7. A catalyst pretreated in syngas ($H_2$/CO = 1.0) has low initial activity and maximum activity, but deactivates after reaching peak activity; the activity of a catalyst pretreated in $H_2$ is initially high and quickly levels off to a moderate steady-state activity; activity of a CO pretreated catalyst is initially low but increases gradually to a moderately high value; the activity of this catalyst continues to increase after 200 hours of testing.
8. The $CH_4$ selectivity of the unpromoted iron catalyst is unexpectedly the lowest among the three catalysts tested. The higher $CH_4$ selectivities for Pt promoted Fe catalyst may be due to a higher hydrogenation activity, which is important in maintaining a clean metal surface and thus preventing fast deactivation

## REFERENCES

Bukur, D. B., Lang, X., A precipitated iron Fischer-Tropsch catalyst for synthesis gas conversion to liquid fuels, *Studies in Surface Science and Catalysis*, 119 (1998), 113-118.

Bukur, D. B., Lang, X., Ding, Y., Pretreatment effect studies with a precipitated iron Fischer-Tropsch catalyst in a slurry reactor, *Applied Catalysis*, 4683 (1999), 1-21.

Huber, G., W., Bartholomew, C. H., Conrad, T. L., Woolley, K. W., Guymon, C. G., Pt promotion of $Co/SiO_2$ Fischer-Tropsch synthesis catalysis, presented at American Chemical Society 219th National Meeting, San Francisco, March 26-30, 2000.

Iglesia, E., Soled, S. L., Fiato, R. A., Via, G. H., Bimetallic Synergy in Cobalt-Ruthenium Fischer-Tropsch Synthesis Catalysts, *Journal of Catalysis*, 143 (1993), 345-368.

Pham, H., Attrition and SEM data, Unpublished Report, August 18, 1999.

Pham, H., Personal Communication, Feb 2000.

Table 3. Catalyst codes and compositions determined by atomic absorption

| Catalyst Code[a] | Support | Fe wt% | K wt% | Pt wt% | Al wt% |
|---|---|---|---|---|---|
| Fe-S-201 | Davisil 644 | 10.7 | - | - | - |
| Fe-S-202 | Davisil 635 | - | - | - | - |
| FePt-S-203 | Davisil 635 | - | - | 0.5[a] | - |
| Fe-S-206 | Davisil 644 | 10.05 | - | - | - |
| FePt-S-206 | Davisil 644 | - | - | - | - |
| Fe-S-207 | Davisil 644 | - | - | - | - |
| FePtK-S-209 |  | 11.11 | 0.21 | 1.53 | - |
| FePtKAl-S-212 |  | 10.36 | 0.46 | 0.38 | - |
| FePtK-215 after fixed bed run[b] |  | 6.82 | 0.53 | 0.45 | - |
| FePtK-S-216 |  | 11.4 | 0.93 | 1.01 | - |
| FePtK-S-217 |  | 11.1 | 0.88 | 0.90 | - |
| FePtK-216 after fixed bed run[b] |  | 6.39 | 0.38 | 0.48 | - |
| FePtK-S-218 |  | 9.25 | - | - | - |
| FePt-S-220 |  | 11.54 | - | - | - |

[a] Calcined catalysts contain about 10-12% Fe, 0.2-0.9% K, 0.5-1.0% Pt, calcined at 200°C for 3 h in flowing He

[b] After reaction, wax removed

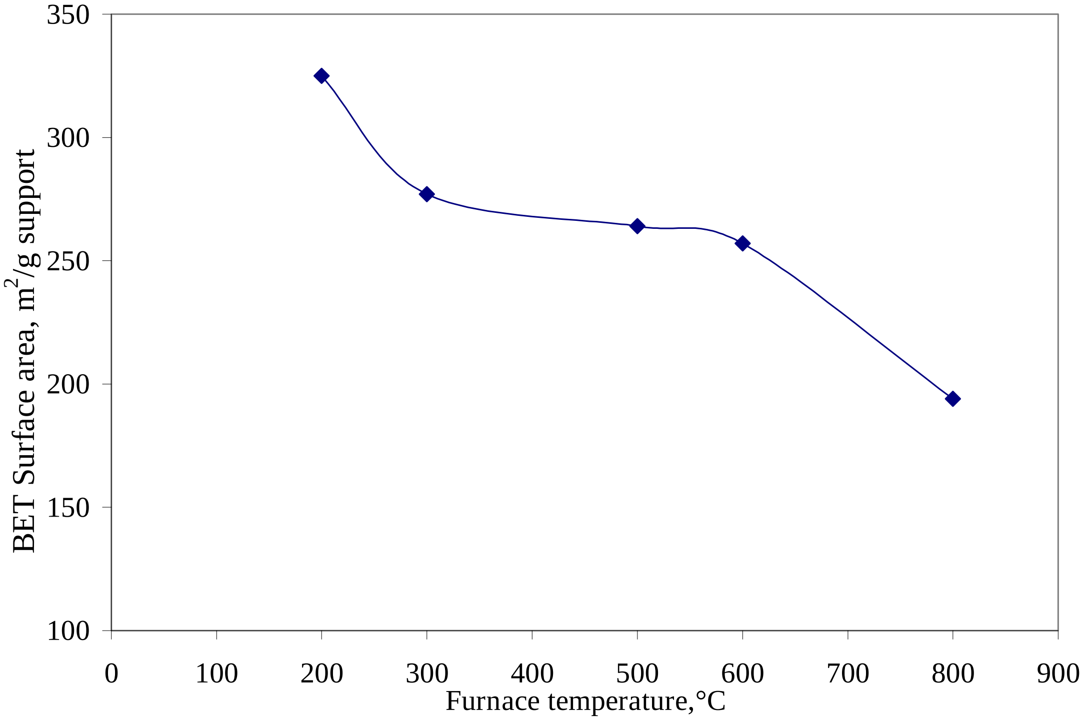

Fig 1. Thermal stability of Davisil 644 support after heating in air for 24 h at different temperatures.

Table 4. BET surface area of catalysts Davisil supported on 635[a] and Davisil 644[b]

| Catalyst Code | Treatment or Test Runs | BET Surface Area m$^2$/g | |
|---|---|---|---|
| | | Run #1 | Run #2 |
| Fe-S-203[a] | After dried @80°C, 24 h | 244 | - |
| FePt-S-203[a] | After dried @80°C, 24 h, | 241 | - |
| Fe-S-206[b] | After 55 h fixed bed run T=270°C P=150psi, wax not removed | 67 | - |
| FePt-S-206[b] | After 140 h fixed bed run, wax not removed | 45 | - |
| FePt-S-209[b] | Fresh catalyst | 266 | - |
| FePt-S-209[b] | After fixed bed run and wax not removed | 7.5 | - |
| FePtK-S-213[b] | After fixed bed run and wax removed in toluene solvent | 240 | 208 |
| FePtK-S-215[b] | Fixed Bed Run and Wax not removed | 145 | - |
| FePtK-S-215[b] | Fixed Bed Run and Soxhlet Wax Removal | 236 | 222 |
| FePtK-S-216[b] | Fresh catalyst calcined in He @200°C | 296 | - |
| FePtK-S-216[b] | Fixed Bed Run and Soxhlet Wax Removal | 225 | - |

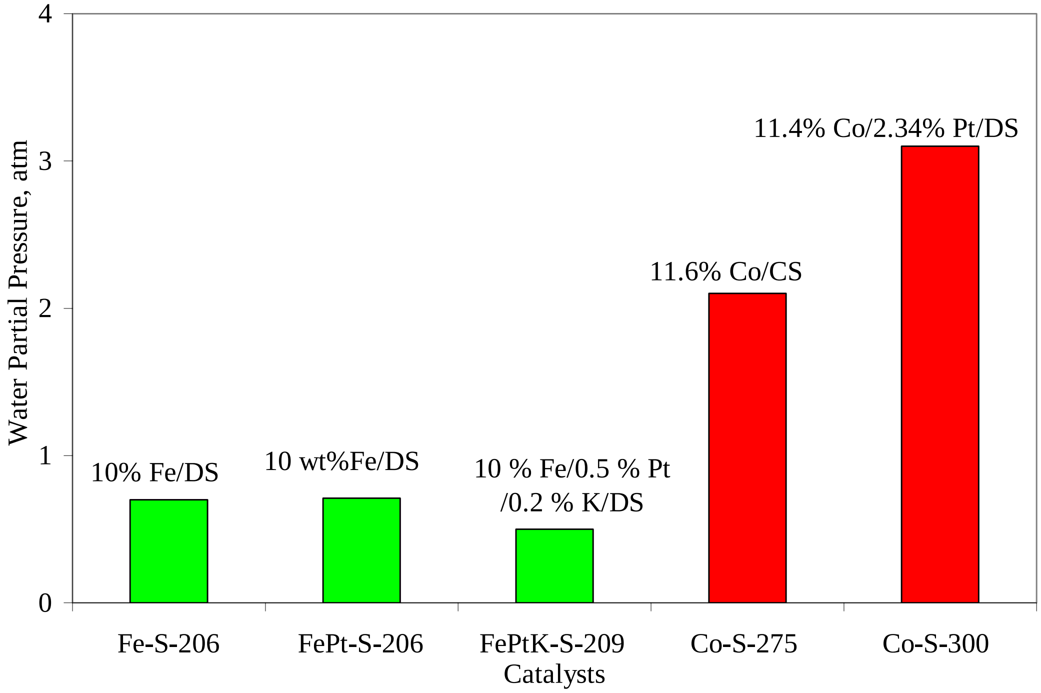

Fig 2. Calculated Water Partial Pressures at Fixed Bed Run Conditions (DS = Davisil 644, CS = Cab-O-Sil)

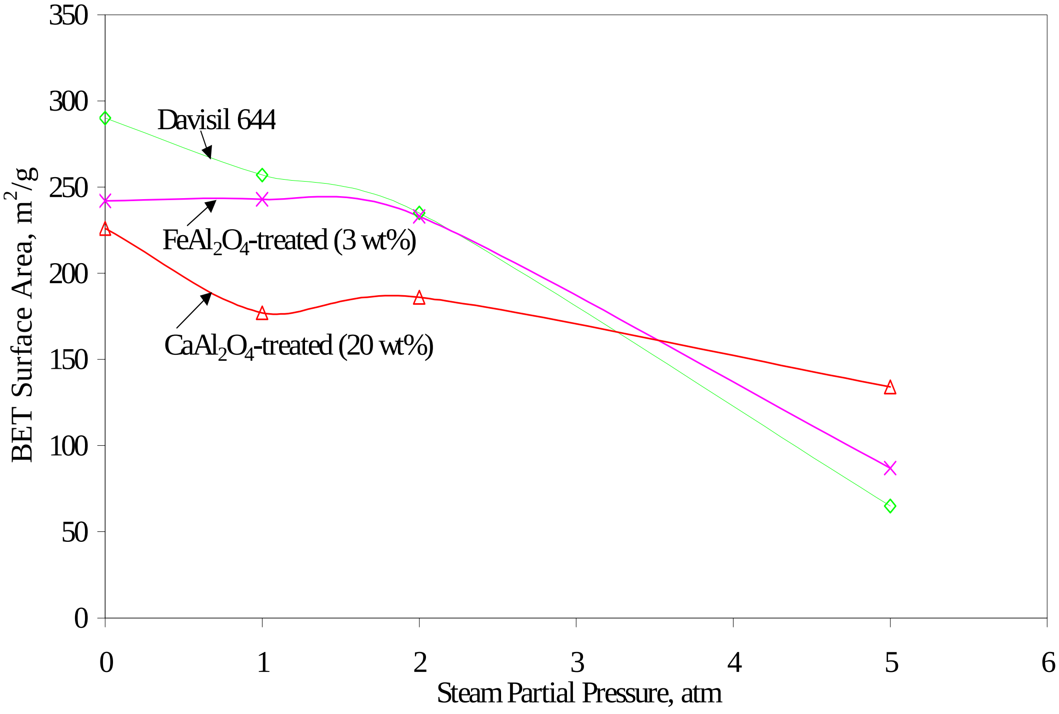

Fig 3. Hydrothermal Stability of Davisil 644 Silica support and $FeAl_2O_4$ Modified Davisil 644 Support (72 h steam treatment at $P_{total}$=10 atm, T=265°C, repeat every run) BET Surface Area Thermal Stability of Davisil 644

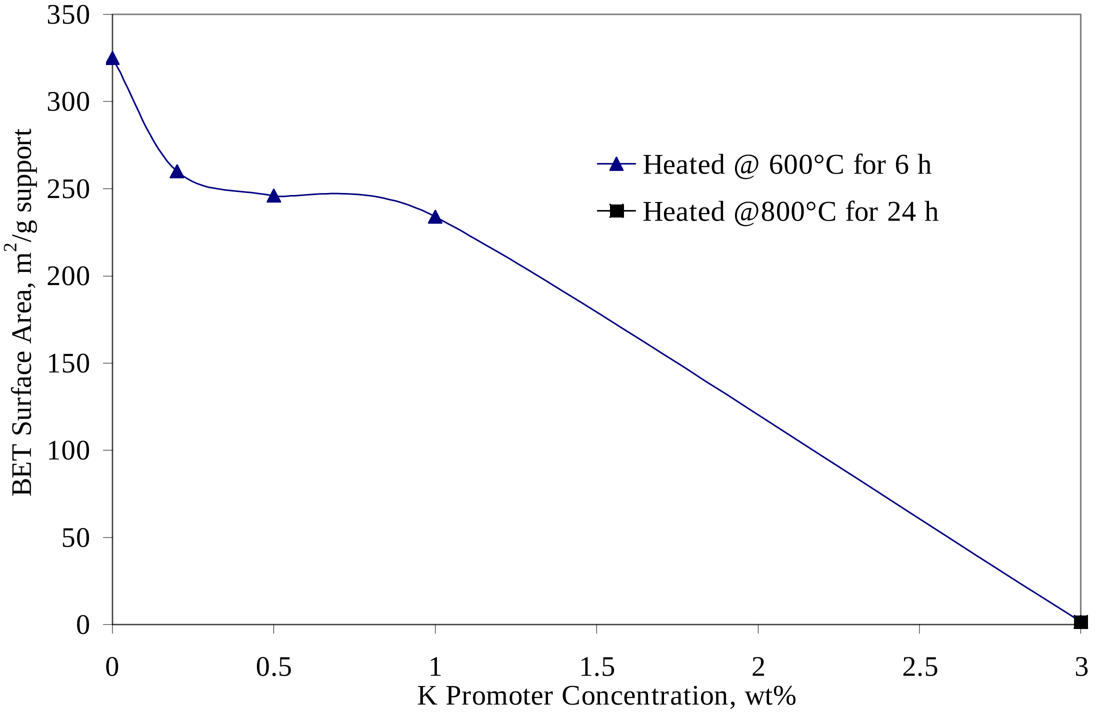

Fig 4. K Promoter Effects on BET Thermal Stability of Davisil 644

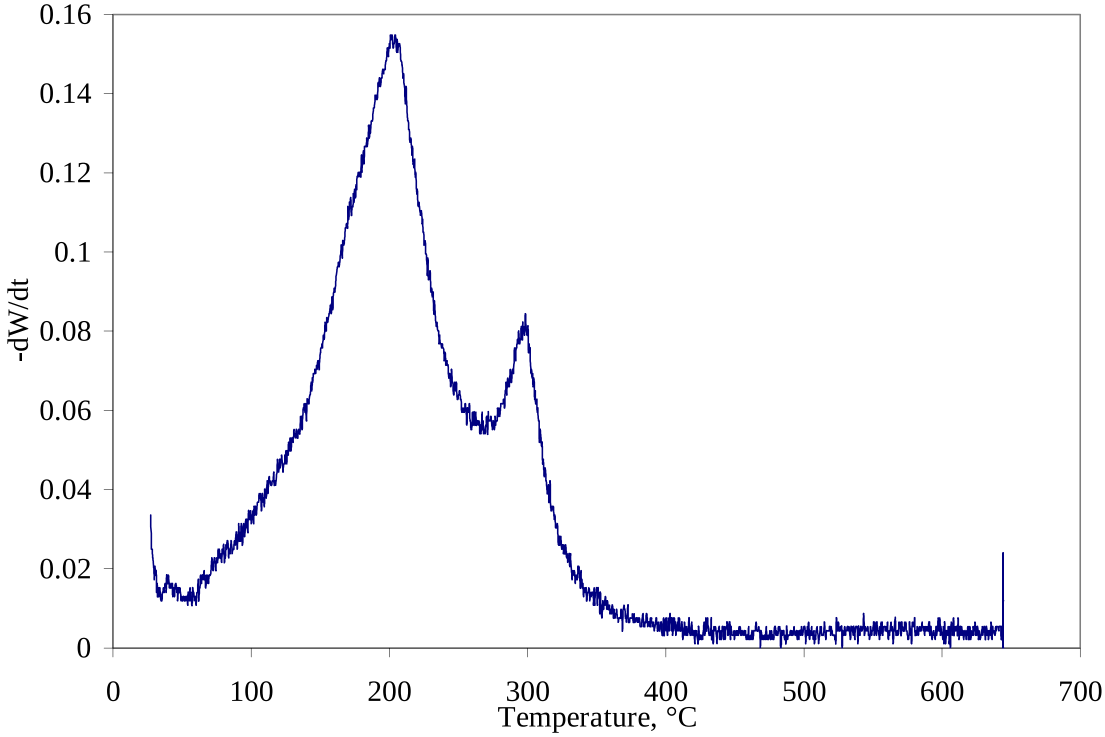

Fig 5. TPAr of Fe-S-207 after drying at 80°C 24 h

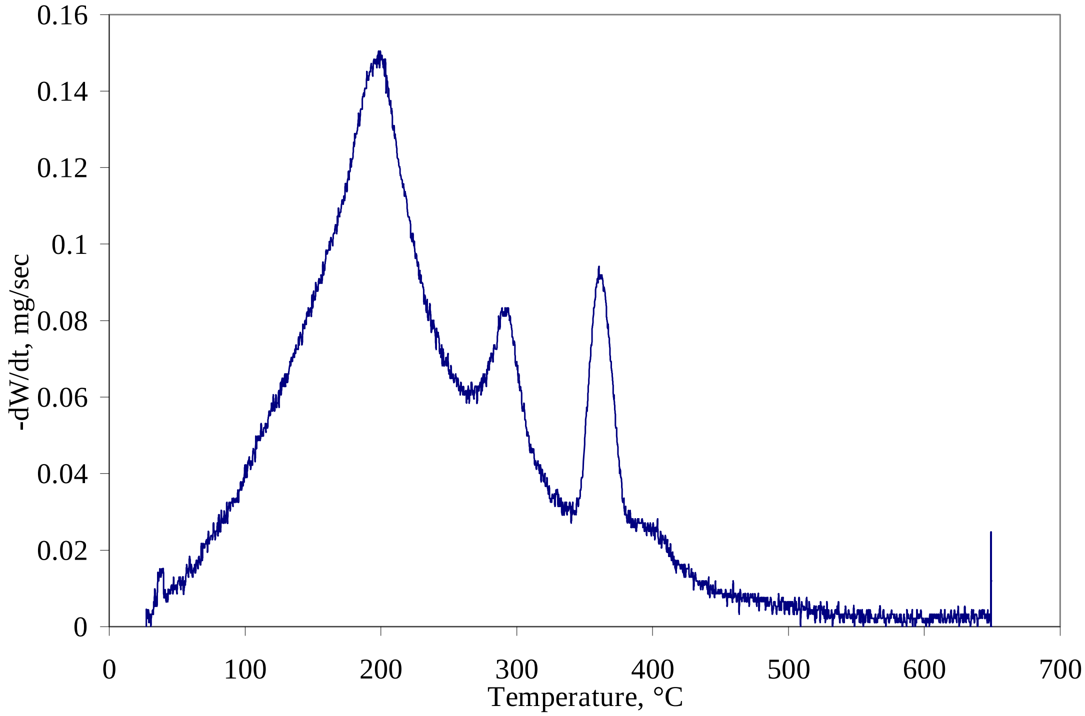

Fig 6. TPR of Fe-S-207 fresh catalyst after drying at 80°C for 24 h

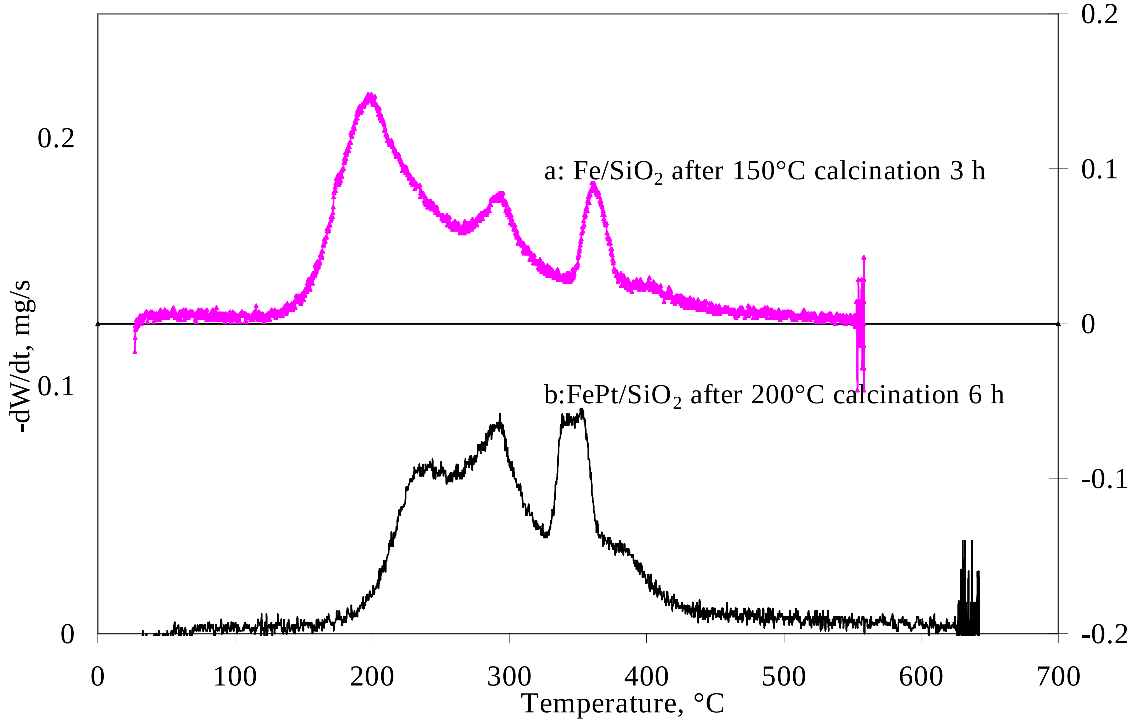

Fig 7. TPR of calcined Fe-S-207 and FePt-S-207

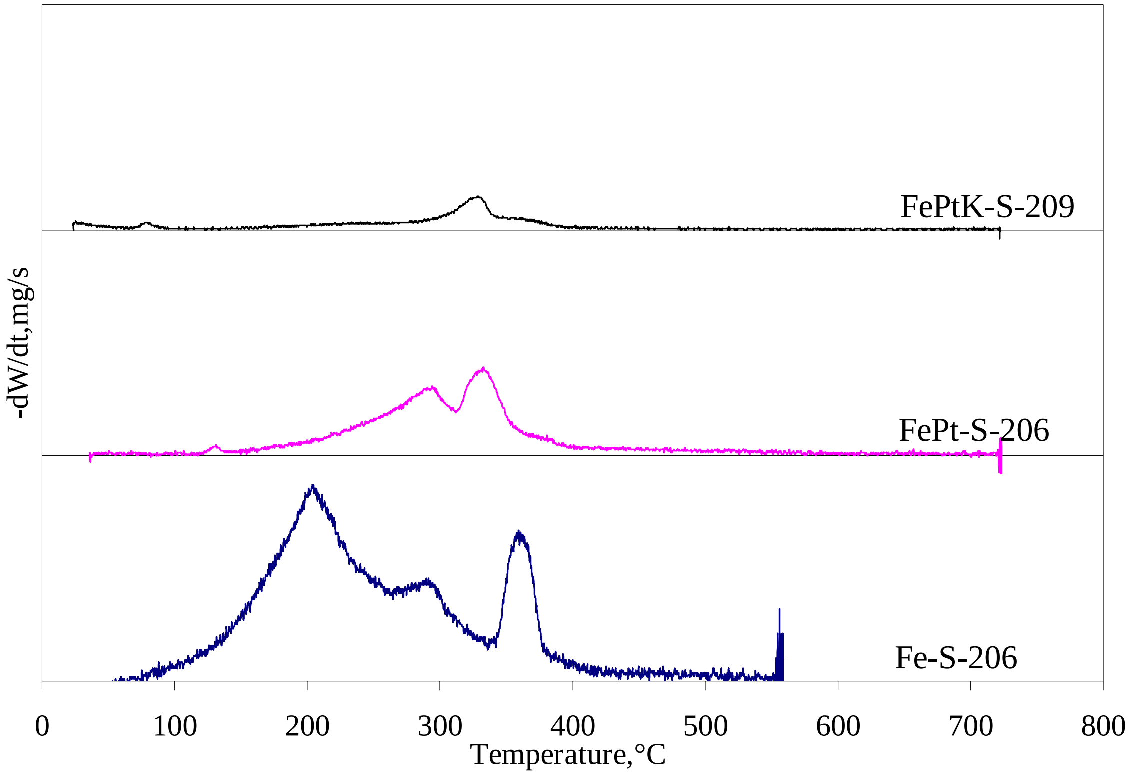

Fig 8. TPR of Unpromoted and Promoted Fe Catalysts after 150°C 3 h calcinations

## Table 5. $H_2$ Chemisorption and Dispersion Measurements

| Catalyst Code | Extent of Reduction at 300°C (%)[a] | $H_2$ Uptake (µmole/gm catalyst) | Dispersion (%) |
|---|---|---|---|
| Fe-S-201 (calcined[b]) | 80 | 41.5 | 7.2 |
| | | 44.1 | 7.7 |
| | | 47.9 | 8.3 |
| Average/Standard Deviation | | 44.5 ± 3.2 | 7.7 ± 0.6 |
| Fe-S-201 after FBR run 01 and wax extraction | 80 | 71.3 | 12.4 |
| | | 50.3 | 8.8 |
| | | 69.2 | 12.0 |
| | | 47.5 | 8.3 |
| Average/Standard Deviation | | 59.6 ± 12.4 | 10.4 ± 2.1 |
| Fe-S-201 after FBR run 08 and wax extraction | 80 | 52.8 | 7.4 |
| | | 52.9 | 7.4 |
| | | 36.4 | 5.1 |
| | | 54.5 | 7.6 |
| Average/Standard Deviation | | 49.1 ± 8.5 | 6.9 ± 1.2 |
| FePt-S-220 (calcined[b]) | 80(Fe), 100(Pt) | 67.7 | 8.6 |
| | | 46.9 | 5.9 |
| | | 38.7 | 4.9 |
| Average/Standard Deviation | | 51.1 ± 14.9 | 6.5 ± 1.9 |
| FePt-S-220 after FBR run 09 and wax extraction | 80(Fe), 100(Pt) | 71.0 | 9.0 |
| | | 116.8 | 14.8 |
| | | 38.7 | 4.9 |
| Average/Standard Deviation | | 75.5 ± 39.2 | 9.6 ± 5.0 |
| FePtK-S-218 (calcined[b]) | 80(Fe), 100(Pt) | 64.1 | 8.1 |
| | | 67.0 | 8.5 |
| | | 38.4 | 4.9 |
| Average/Standard Deviation | | 56.5 ± 15.7 | 7.2 ± 2.0 |
| FePtK-S-218 after FBR run 05 and wax extraction | 80(Fe), 100(Pt) | 173.2 | 22.0 |
| | | 48.3 | 6.1 |
| | | 92.6 | 11.8 |
| Average/Standard Deviation | | 104.7 ± 63.3 | 13.3 ± 8.0 |
| FePtK-S-218 after FBR run 07 and wax extraction | 80(Fe), 100(Pt) | 180.1 | 25.1 |
| | | 218.0 | 30.4 |
| | | 36.4 | 5.1 |
| | | 47.1 | 6.6 |
| Average/Standard Deviation | | 120.4 ± 92.2 | 16.8 ± 12.9 |

[a] Estimated value measured by TPR.

[b] Catalyst calcined at 200°C in He for 3 h.

[c] $H_2$ reduction profile: increase at 1°C/min from room temperature to 300°C and keep 16 h.

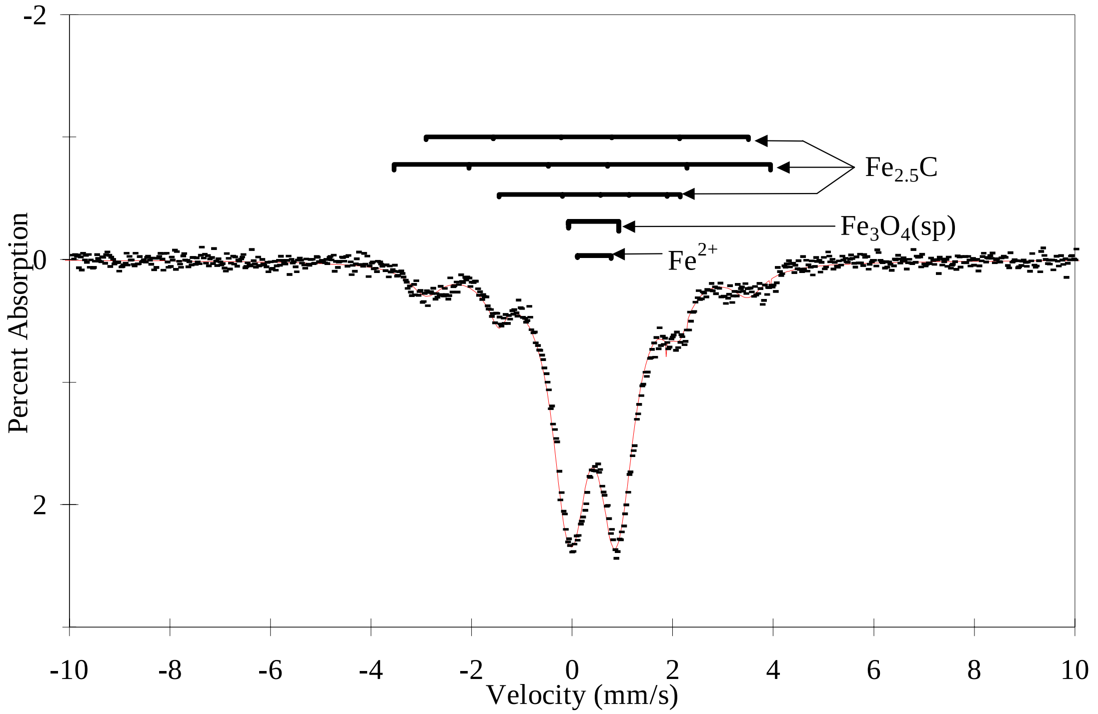

Fig 9. Fe-S-206 After 55hrs fixed bed test run

Table 6. Mössbauer spectroscopy parameters of Fe-S-206 after 55 h fixed bed run at 270°C,10 atm, $H_2$/CO=1.

| Species | Iron site | IS[a] mm/s | $\Delta E_Q$[b] mm/s | HFS KOe | % Area 298 K | % Area 77 K |
|---|---|---|---|---|---|---|
| 10 wt% Fe/$SiO_2$(Davisil 635) after 55 h fixed bed test at 280°C P=1atm, $H_2$/CO=1. | | | | | | |
| (spectra collected at 298K for 24 h) | | | | | | |
| $Fe_3O_4$ (sp)[c] | | 0.43 | 0.99 | --- | 63.5 | |
| | | 0.44 | 0.67 | --- | 10.9 | |
| $\chi$-$Fe_{2.5}C$ | I | 0.29 | 0.02 | 198 | 18.0 | |
| | II | 0.16 | 0.09 | 232 | 0.05 | |
| | III | 0.60 | -0.50 | 111 | 7.6 | |
| $Fe^{2+}$ | | 0.68 | 2.39 | --- | 0.06 | |

[a] Relative to $\alpha$-Fe.

[b] For magnetically split spectra this value is $2\varepsilon'$ ,$\Delta E_Q=2\varepsilon'$ if$\phi=0$.

[c] Superparamagnetic $Fe_3O_4$.

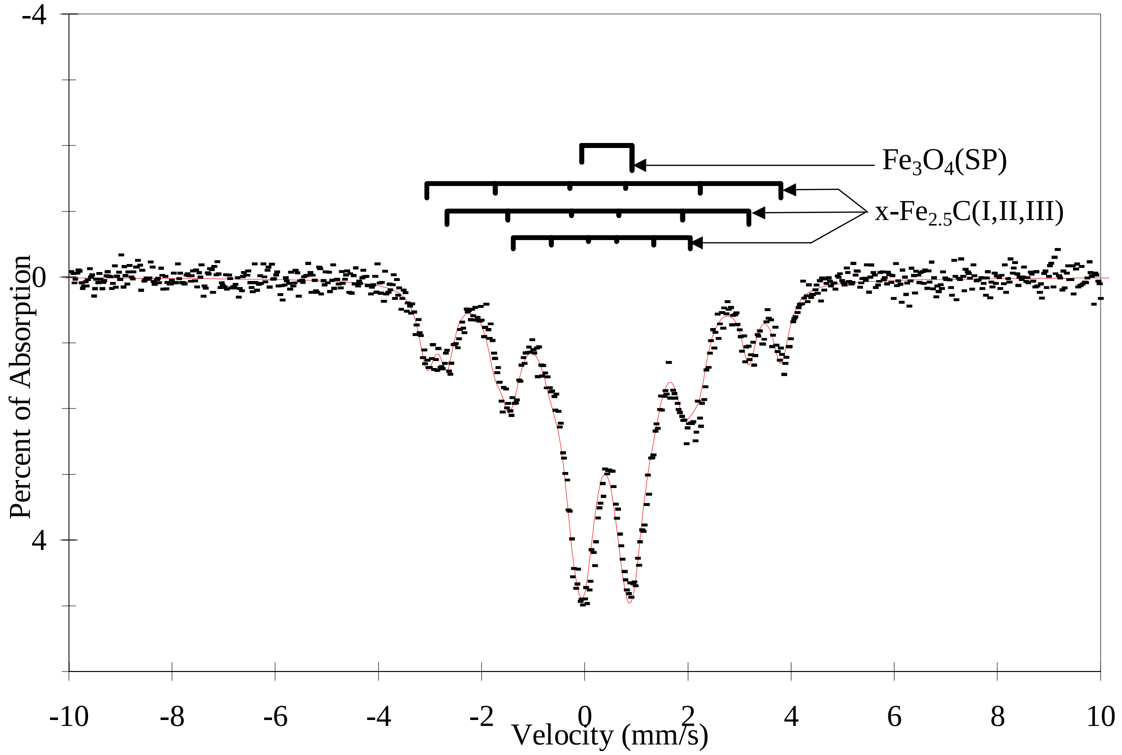

Fig 10. FePt-S-203 after fixed bed run (spectra collected at 298 K)

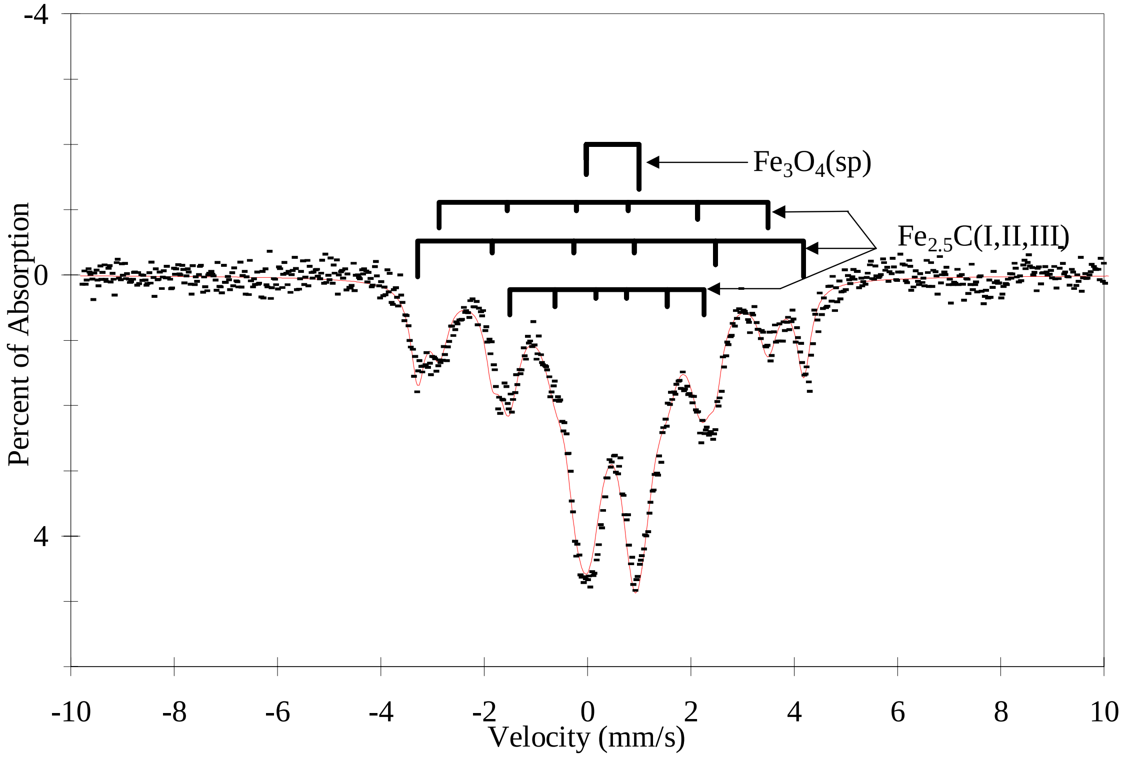

Fig 11. FePt-S-203 after fixed bed run (spectra collected at 77K)

Table 7. Room Temperature and Liquid $N_2$ Temperature Mössbauer spectroscopy parameters of FePt-S-203 catalyst after fixed bed run at 270°C,10 atm, $H_2$/CO=1

| Species | Iron site | IS[a] mm/s | $\Delta E_Q$[b] mm/s | HFS KOe | % Area 298 K | % Area 77 K |
|---|---|---|---|---|---|---|
| 10 wt% Fe/0.5 wt% Pt/$SiO_2$(Davisil 644) after 60 h fixed bed test | | | | | | |
| (spectra collected at 298K for 24 h) | | | | | | |
| $Fe_3O_4$ (sp)[c] | | 0.43 | 0.97 | --- | 50.6 | |
| $\chi$-$Fe_{2.5}C$ | I | 0.23 | 0.05 | 181 | 14.7 | |
| | II | 0.31 | 0.12 | 212 | 17.8 | |
| | III | 0.34 | -0.02 | 106 | 16.8 | |
| 10 wt% Fe/0.5 wt% Pt/$SiO_2$(Davisil 644) after 60 h fixed bed test | | | | | | |
| (spectra collected at 77K for 24 h) | | | | | | |
| $Fe_3O_4$ (sp)[c] | | | | | | |
| $\chi$-$Fe_{2.5}C$ | | 0.49 | 1.02 | --- | | 48.6 |
| | I | 0.30 | 0.02 | 197 | | 16.5 |
| | II | 0.39 | 0.13 | 231 | | 17.6 |
| | III | 0.42 | -0.08 | 117 | | 17.4 |

[a] Relative to $\alpha$-Fe.

[b] For magnetically split spectra this value is $2\varepsilon'$ ,$\Delta E_Q=2\varepsilon'$ if$\phi=0$.

[c] Superparamagnetic $Fe_3O_4$.

Table 8. Iron phases of unpromoted (Fe-S-206) and promoted (FePt-S-203, FePtK-S-218) catalysts (room temperature and liquid $N_2$ Mössbauer Spectra)

| Catalyst | Temp[a] K | Iron species % Area | | | |
|---|---|---|---|---|---|
| | | $Fe_3O_4$ (FiM)[b] | $Fe_{2.5}C$[c] | $Fe^{2+}$ | $Fe_3O_4$ (sp) |
| Fe-S-206 | 298 | - | 25.6 | 0.1 | 74.3 |
| FePt-S-203 | 298 | - | 49.3 | - | 50.6 |
| FePt-S-203 | 77 | - | 51.5 | - | 48.6 |

[a]: Temperatures at which Mössbauer Spectra are collected

[b]: Ferrimagnetic $Fe_3O_4$

[c]: Haag or $\chi$-carbides ($Fe_{2.5}C$)

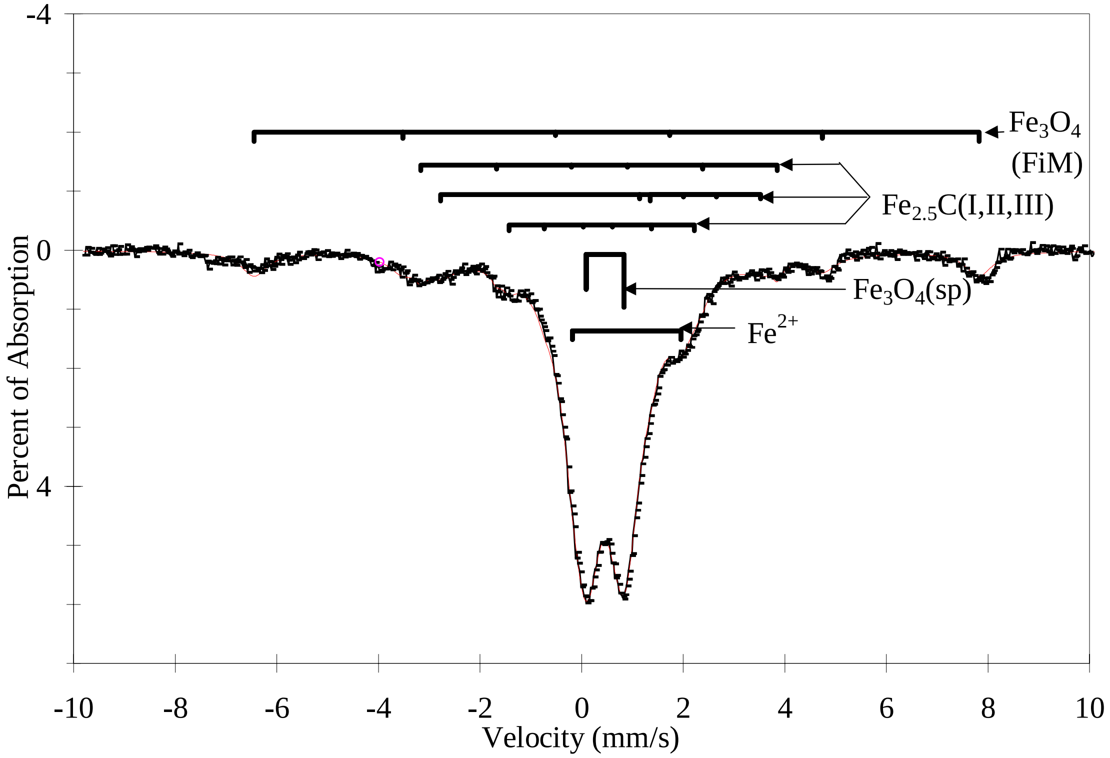

Fig 12. In-situ Mössbauer spectrum of Fe-S-207 after pretreated at 280°C, 1atm and $H_2/CO=1$.

Table 9. Mössbauer spectroscopy parameters of Fe-S-207 after 16 h in-situ pretreatment at 280°C (spectra collected at 298K for 24 h).

| Species | Iron site | IS[c]<br>(mm/s) | $\Delta E_Q$[d]<br>(mm/s) | HFS<br>KOe | % Area |
|---|---|---|---|---|---|
| 10 wt% Fe/$SiO_2$ pretreated in $H_2$/CO 16 h | | | | | |
| $Fe_3O_4$ (FiM[e]) | | 0.65 | 0.08 | 442 | 10.3 |
| $\chi$- $Fe_{2.5}C$ (295K) | I | 0.81 | -0.01 | 128 | 8.1 |
| | II | 0.35 | -3.04 | 217 | 2.3 |
| | III | 0.36 | 0.08 | 113 | 3.6 |
| $Fe^{2+}$ (295K) | | 0.89 | 2.14 | --- | 7.5 |
| $Fe_3O_4$ (sp)[f] | | 0.46 | 0.74 | --- | 68.2 |

[a] Catalyst preparation and composition similar to Fe-S-206

[b] In-situ treatment was conducted at 1 atm; gas largely bypassed the sample leading to low extent of carbide formation

[c] Relative to $\alpha$-Fe.

[d] For magnetically split spectra this value is $2\varepsilon'$ ,$\Delta E_Q=2\varepsilon'$ if $\phi=0$.

[e] Ferrimagnetic $Fe_3O_4$.

[f] Superparamagnetic $Fe_3O_4$.

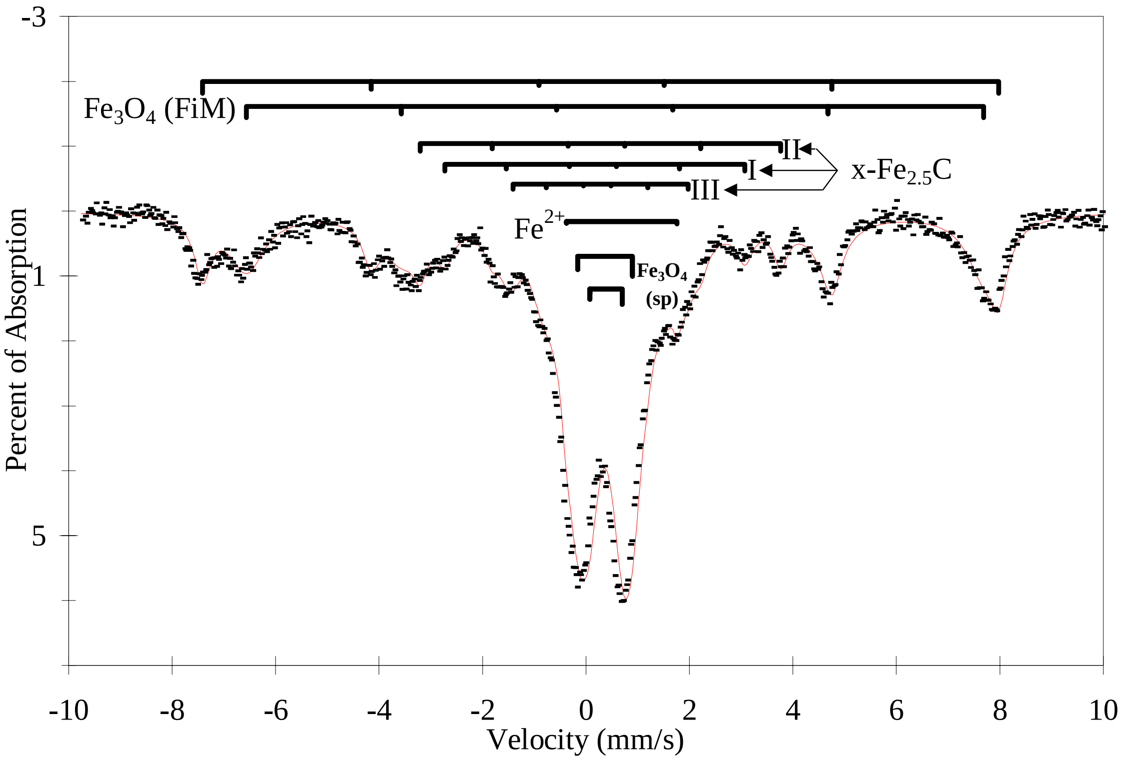

Fig 13. Mossbauer Spectrum of Fe-S-201 (10.7 % Fe/$SiO_2$) after statistically designed experiments run #01

| | |
|---|---|
| SCA settings: | Source to Counter distance: 7 inch |
| Window: 0.8 volts | Count rate:15,616 counts/sec |
| Lower level: 5.6 volts | Data collected at room temperature |
| Course gain: 1 K | for 24 h |
| Fine gain: 0.532 | |

Table 10. Mössbauer spectroscopy parameters of 10.7 wt%Fe/SiO $_2$ catalyst after statistically designed fixed bed run # 01 at 250°C,10 atm, $H_2$/CO=1

| Species | Iron site | IS[a] mm/s | $\Delta E_Q$[b] mm/s | HFS KOe | % Area (298 K) | % Area (77 K) |
|---|---|---|---|---|---|---|
| 10.7 wt% Fe/$SiO_2$ after 150 h fixed bed test at 280°C P=1atm, $H_2$/CO=1<br>(spectra collected at 298K for 24 h) | | | | | | |
| $Fe_3O_4$ (FiM[c]) | | 0.29 | -0.02 | 477 | 11.2 | |
| | | 0.56 | 0.01 | 441 | 22.1 | |
| $\chi$-$Fe_{2.5}C$ | I | 0.15 | 0.04 | 179 | 6.3 | |
| | II | 0.24 | 0.08 | 216 | 6.6 | |
| | III | 0.25 | 0.07 | 105 | 4.6 | |
| $Fe^{2+}$ | | 0.69 | 2.14 | --- | 0.8 | |
| $Fe_3O_4$ (sp)[d] | | 0.37 | 1.1 | --- | 28.4 | |
| | | 0.39 | 0.6 | --- | 20.0 | |

[a] Relative to $\alpha$-Fe.

[b] For magnetically split spectra this value is $2\varepsilon'$ ,$\Delta E_Q=2\varepsilon'$ if$\phi=0$.

[c] Ferrimagnetic $Fe_3O_4$.

[d] Superparamagnetic $Fe_3O_4$.

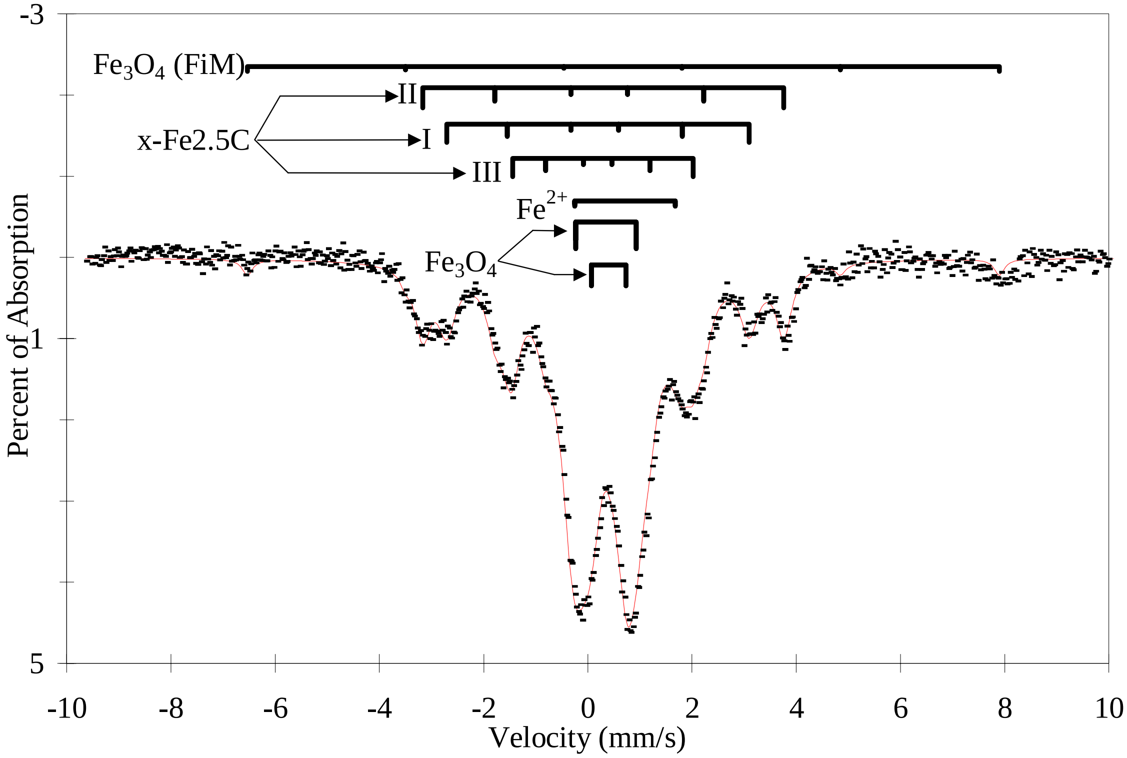

Fig 14. Mossbauer Spectrum of Fe-S-201 (10.7 % Fe/$SiO_2$) after statistically designed experiments run #02

| | |
|---|---|
| SCA settings: | Source to Counter distance: 7 inch |
| Window: 0.8 volts | Count rate:17,932 counts/sec |
| Lower level: 5.6 volts | Data collected at room temperature |
| Course gain: 1 K | for 24 h |
| Fine gain: 0.532 | |

Table 11. Mössbauer spectroscopy parameters of 10.7 wt%Fe/SiO $_2$ catalyst after statistically designed fixed bed run # 02 at 265°C,10 atm, $H_2$/CO=1

| Species | Iron site | IS[a] mm/s | $\Delta E_Q$[b] mm/s | HFS KOe | % Area (298 K) | % Area (77 K) |
|---|---|---|---|---|---|---|
| 10.7 wt% Fe/$SiO_2$ after 150 h fixed bed test at 265°C P=1atm, $H_2$/CO=1<br>(spectra collected at 298K for 24 h) | | | | | | |
| $Fe_3O_4$ (FiM[c]) | | 0.68 | 0.01 | 446 | 2.2 | |
| $\chi$-$Fe_{2.5}C$ | I | 0.16 | 0.06 | 180 | 14.7 | |
| | II | 0.26 | 0.08 | 215 | 14.3 | |
| | III | 0.24 | 0.10 | 107 | 12.4 | |
| $Fe^{2+}$ | | 0.71 | 1.93 | --- | 5.3 | |
| $Fe_3O_4$ (sp)[d] | | 0.35 | 1.16 | --- | 31.2 | |
| | | 0.40 | 0.66 | --- | 20.0 | |

[a] Relative to $\alpha$-Fe.

[b] For magnetically split spectra this value is $2\varepsilon'$ ,$\Delta E_Q=2\varepsilon'$ if$\phi=0$.

[c] Ferrimagnetic $Fe_3O_4$.

[d] Superparamagnetic $Fe_3O_4$.

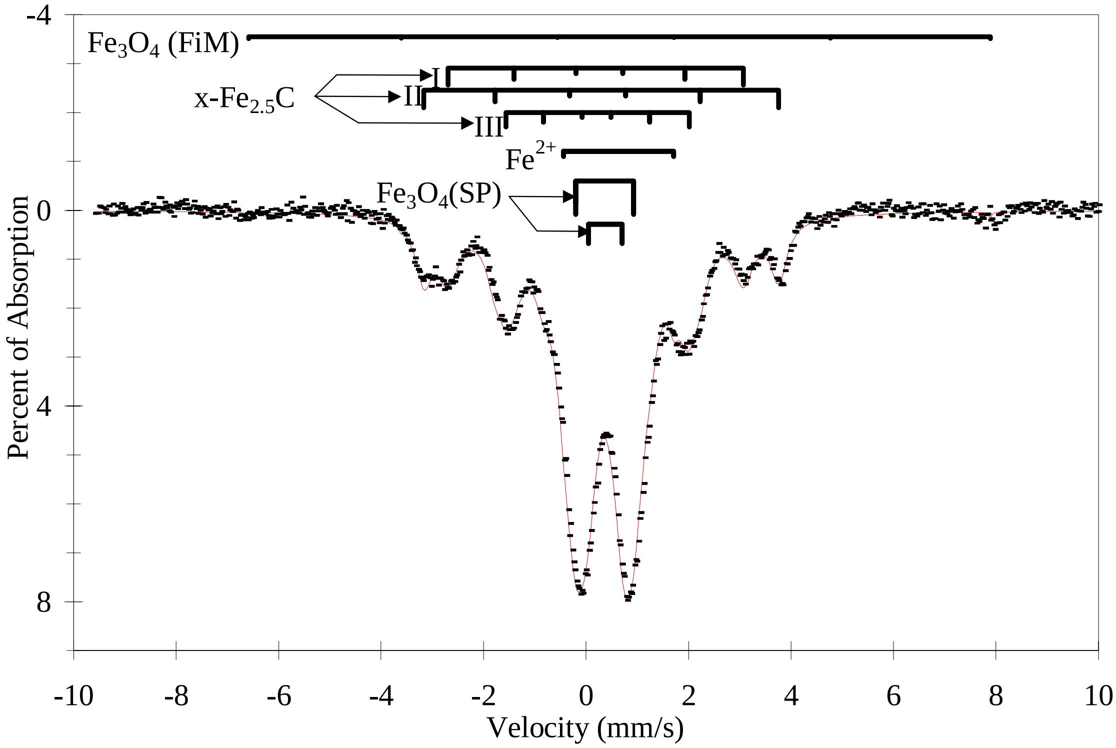

Fig 15. Mossbauer Spectrum of Fe-S-201 (10.7 % Fe/SiO$_2$) after statistically designed experiments run #03

SCA settings:
Window: 0.8 volts
Lower level: 5.6 volts
Course gain: 1 K
Fine gain: 0.532

Source to Counter distance: 7 inch
Count rate:14,300 counts/sec
Data collected at room temperature for 24 h

Table 12. Mössbauer spectroscopy parameters of 10.7 wt%Fe/$SiO_2$ catalyst after statistically designed fixed bed run # 03 at 250°C,10 atm, $H_2$/CO=1

| Species | Iron site | IS[a] mm/s | $\Delta E_Q$[b] mm/s | HFS KOe | % Area (298 K) | % Area (77 K) |
|---|---|---|---|---|---|---|
| 10.7 wt% Fe/$SiO_2$ after 150 h fixed bed test at 265°C P=1atm, $H_2$/CO=1<br>(spectra collected at 298K for 24 h) | | | | | | |
| $Fe_3O_4$ (FiM[c]) | | 0.62 | 0.07 | 448 | 0.24 | |
| $\chi$-$Fe_{2.5}C$ | I | 0.22 | -0.07 | 179 | 16.5 | |
| | II | 0.26 | 0.07 | 214 | 13.5 | |
| | III | 0.21 | 0.02 | 111 | 11.2 | |
| $Fe^{2+}$ | | 0.64 | 2.15 | --- | 2.7 | |
| $Fe_3O_4$ (sp)[d] | | 0.36 | 1.13 | --- | 38.0 | |
| | | 0.38 | 0.66 | --- | 18.0 | |

[a] Relative to $\alpha$-Fe.

[b] For magnetically split spectra this value is $2\varepsilon'$ ,$\Delta E_Q=2\varepsilon'$ if$\phi=0$.

[c] Ferrimagnetic $Fe_3O_4$.

[d] Superparamagnetic $Fe_3O_4$.

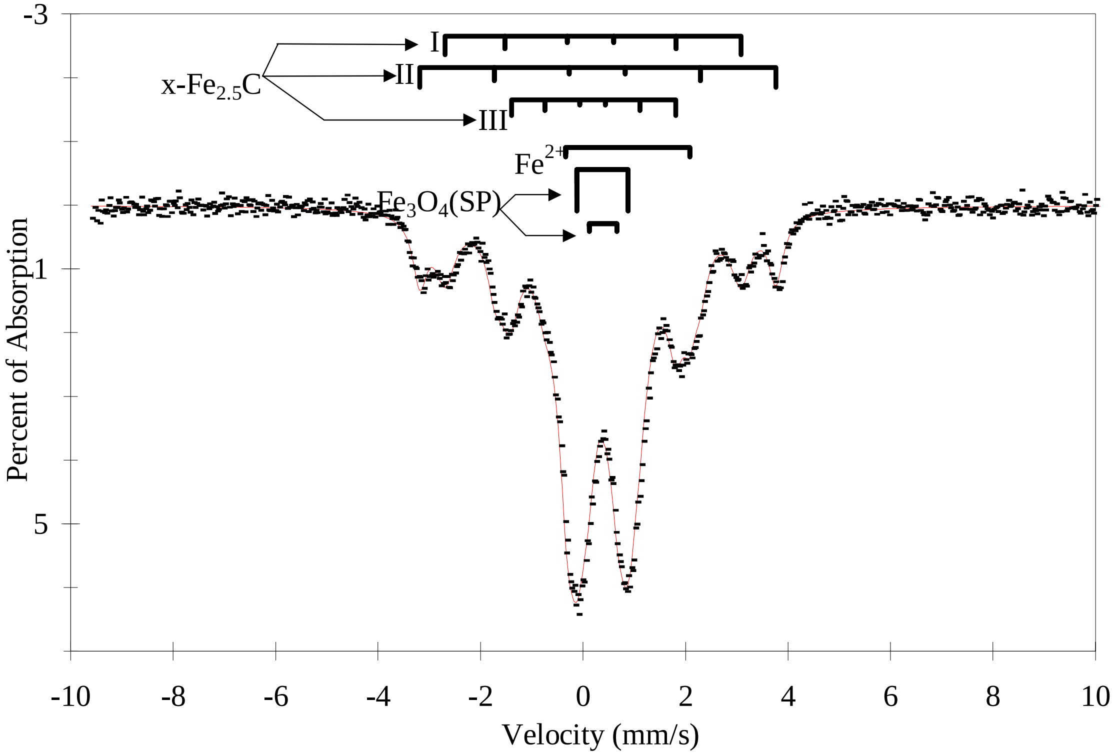

Fig 16. Mossbauer Spectrum of FePt-S-220 after statistically designed experiments run #04

SCA settings:
Window: 0.8 volts
Lower level: 5.6 volts
Course gain: 1 K
Fine gain: 0.532

Source to Counter distance: 7 inch
Count rate:15,640 counts/sec
Data collected at room temperature
for 24 h

Table 13. Mössbauer spectroscopy parameters of FePt-S-220 catalyst after statistically designed fixed bed run # 04 at 250°C,10 atm, $H_2$/CO=1;Catalyst pretreated in H2/CO=0.1, 280°C for 16 h

| Species | Iron site | IS[a] mm/s | $\Delta E_Q$[b] mm/s | HFS KOe | % Area (298 K) | % Area (77 K) |
|---|---|---|---|---|---|---|
| FePt-S-220 after 150 h<br>fixed bed test at 250°C P=1atm, $H_2$/CO=1<br>(spectra collected at 298K for 24 h) | | | | | | |
| $\chi$-$Fe_{2.5}C$ | I | 0.17 | 0.05 | 179 | 16.6 | |
| | II | 0.28 | 0.01 | 215 | 12.7 | |
| | III | 0.20 | 0.03 | 99 | 11.8 | |
| $Fe^{2+}$ | | 0.87 | 2.42 | --- | 5.8 | |
| $Fe_3O_4$ (sp)[c] | | 0.38 | 0.99 | --- | 48.4 | |
| | | 0.39 | 0.54 | --- | 4.6 | |

[a] Relative to $\alpha$-Fe.

[b] For magnetically split spectra this value is $2\varepsilon'$ ,$\Delta E_Q=2\varepsilon'$ if$\phi=0$.

[c] Superparamagnetic $Fe_3O_4$.

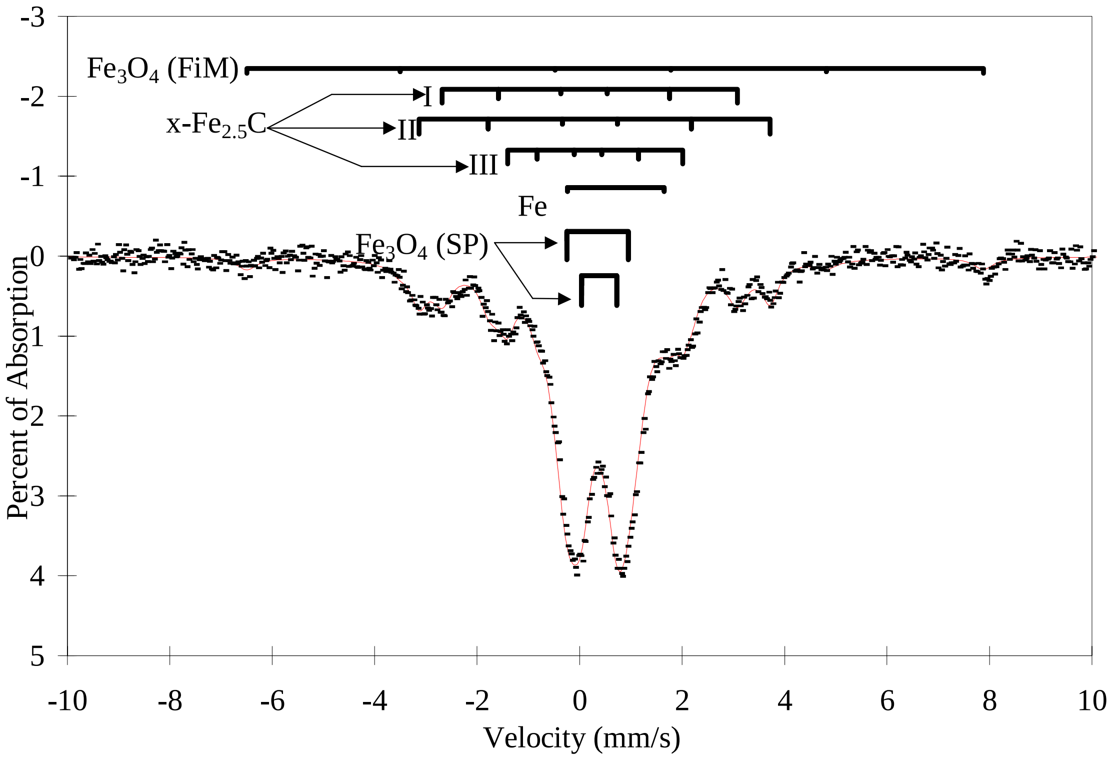

Fig 17. Mossbauer Spectrum of FePtK-S-218 after statistically designed experiments run #05

SCA settings:
Window: 0.8 volts
Lower level: 5.6 volts
Course gain: 1 K
Fine gain: 0.532

Source to Counter distance: 7 inch
Count rate:18,253 counts/sec
Data collected at room temperature
for 24 h

Table 14. Mössbauer spectroscopy parameters of FePtK-S-218 catalyst after statistically designed fixed bed run # 05 at 265°C,10 atm, $H_2$/CO=1

| Species | Iron site | IS[a] mm/s | $\Delta E_Q$[b] mm/s | HFS KOe | % Area (298 K) | % Area (77 K) |
|---|---|---|---|---|---|---|
| FePtK-S-218 after 150 h<br>fixed bed test at 265°C P=1atm, $H_2$/CO=1<br>(spectra collected at 298K for 24 h) | | | | | | |
| $Fe_3O_4$ (FiM[c]) | | 0.67 | 0.04 | 445 | 4.0 | |
| $\chi$-$Fe_{2.5}C$ | I | 0.14 | 0.11 | 179 | 12.6 | |
| | II | 0.25 | 0.09 | 212 | 10.6 | |
| | III | 0.23 | 0.14 | 106 | 8.6 | |
| $Fe^{2+}$ | | 0.71 | 1.89 | --- | 4.8 | |
| $Fe_3O_4$ (sp)[d] | | 0.35 | 1.20 | --- | 30.4 | |
| | | 0.38 | 0.69 | --- | 29.0 | |

[a] Relative to $\alpha$-Fe.

[b] For magnetically split spectra this value is $2\varepsilon'$ ,$\Delta E_Q=2\varepsilon'$ if$\phi=0$.

[c] Ferrimagnetic $Fe_3O_4$.

[d] Superparamagnetic $Fe_3O_4$.

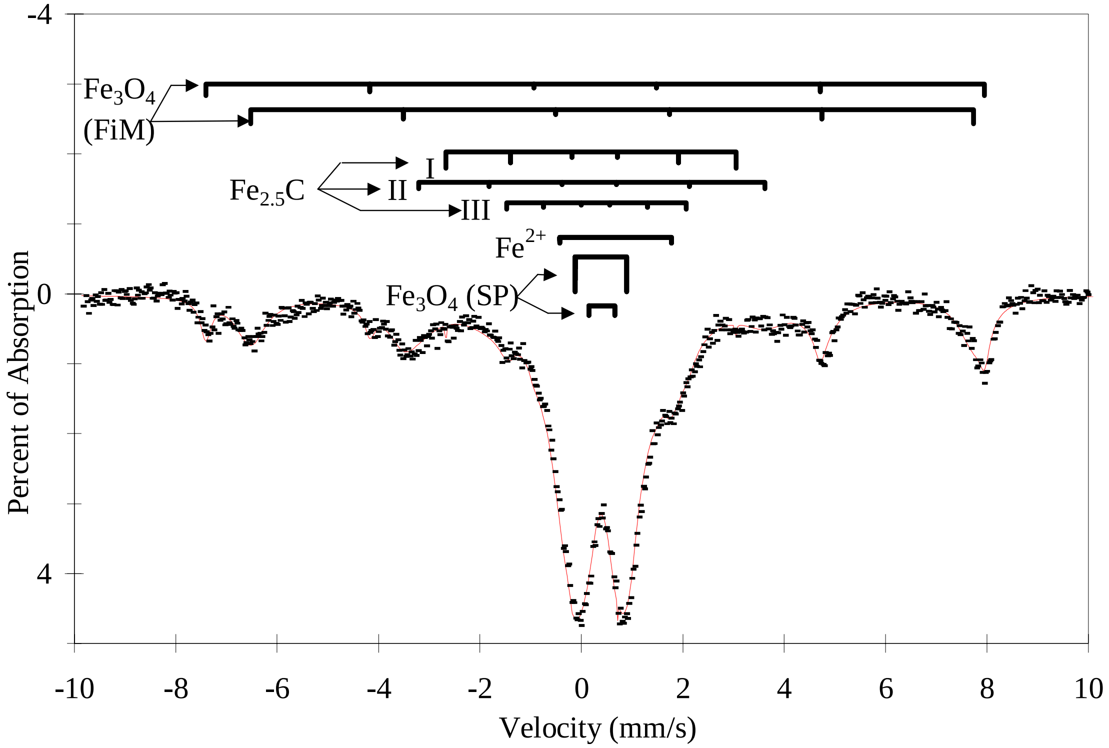

Fig 18. Mossbauer Spectrum of Fe-S-201 after statistically designed experiments run #06

SCA settings:
Window: 0.8 volts
Lower level: 5.6 volts
Course gain: 1 K
Fine gain: 0.532

Source to Counter distance: 7 inch
Count rate:16,620 counts/sec
Data collected at room temperature for 24 h

Table 15. Mössbauer spectroscopy parameters of Fe-S-201 catalyst after statistically designed fixed bed run # 06 at 265°C,10 atm, $H_2$/CO=1

| Species | Iron site | IS[a] mm/s | $\Delta E_Q$[b] mm/s | HFS KOe | % Area (298 K) | % Area (77 K) |
|---|---|---|---|---|---|---|
| Fe-S-201 after 150 h<br>fixed bed test at 265°C P=1atm, $H_2$/CO=1<br>(spectra collected at 298K for 24 h) | | | | | | |
| $Fe_3O_4$ (FiM[c]) | | 0.27 | -0.00 | 475 | 5.6 | |
| | | 0.61 | -0.01 | 441 | 19.0 | |
| $\chi$-$Fe_{2.5}C$ | I | 0.23 | -0.07 | 177 | 0.26 | |
| | II | 0.18 | 0.05 | 211 | 13.8 | |
| | III | 0.29 | 0.02 | 110 | 5.4 | |
| $Fe^{2+}$ | | 0.67 | 2.19 | --- | 4.4 | |
| $Fe_3O_4$ (sp)[d] | | 0.38 | 1.02 | --- | 44.1 | |
| | | 0.40 | 0.51 | --- | 7.5 | |

[a] Relative to $\alpha$-Fe.

[b] For magnetically split spectra this value is $2\varepsilon'$ ,$\Delta E_Q=2\varepsilon'$ if$\phi=0$.

[c] Ferrimagnetic $Fe_3O_4$.

[d] Superparamagnetic $Fe_3O_4$.

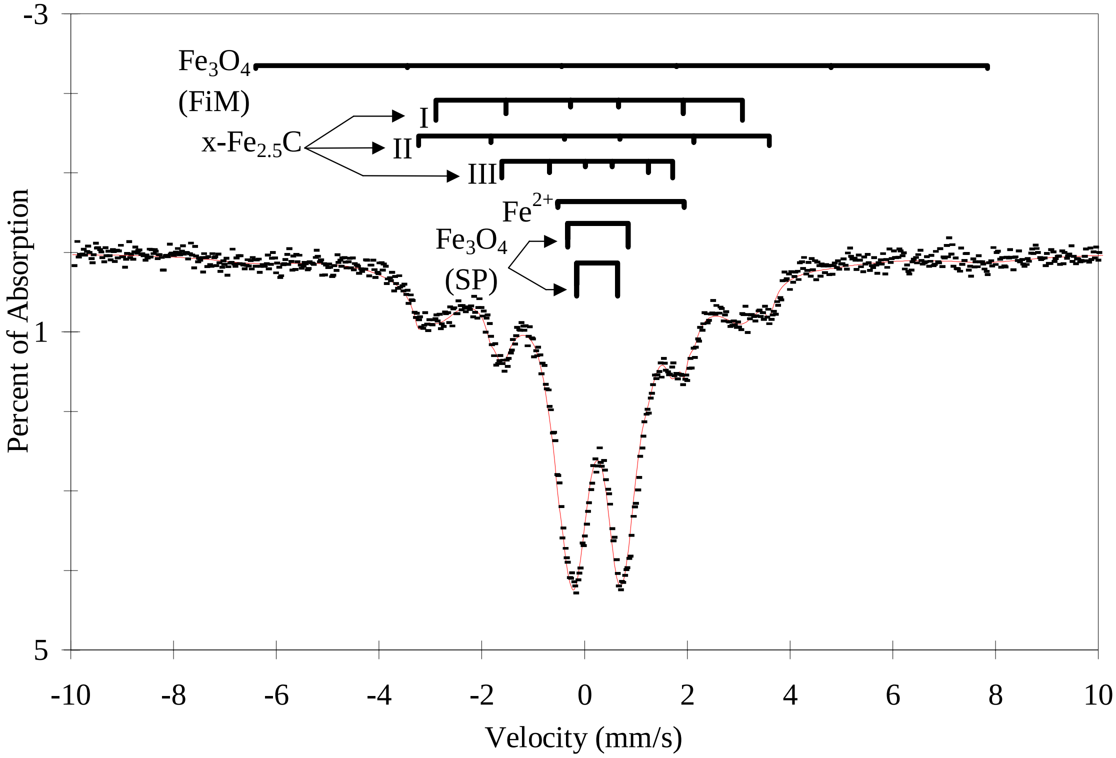

Fig 19. Mossbauer Spectrum of FePtK-S-218 after statistically designed experiments run #07

| | |
|---|---|
| SCA settings: | Source to Counter distance: 7 inch |
| Window: 0.8 volts | Count rate:19,489 counts/sec |
| Lower level: 5.6 volts | Data collected at room temperature |
| Course gain: 1 K | for 24 h |
| Fine gain: 0.532 | |

Table 16. Mössbauer spectroscopy parameters of FePtK-S-218 catalyst after statistically designed fixed bed run # 07 at 265°C,10 atm, $H_2$/CO=1

| Species | Iron site | IS[a] mm/s | $\Delta E_Q$[b] mm/s | HFS KOe | % Area (298 K) | % Area (77 K) |
|---|---|---|---|---|---|---|
| FePtK-S-218 after 150 h<br>fixed bed test at 265°C P=1atm, $H_2$/CO=1<br>(spectra collected at 298K for 24 h) | | | | | | |
| $Fe_3O_4$ (FiM[c]) | | 0.70 | 0.05 | 441 | 7.7 | |
| $\chi$-$Fe_{2.5}C$ | I | 0.14 | -0.11 | 185 | 32.3 | |
| | II | 0.17 | 0.04 | 212 | 3.1 | |
| | III | 0.17 | 0.14 | 103 | 8.8 | |
| $Fe^{2+}$ | | 0.71 | 1.89 | --- | 1.3 | |
| $Fe_3O_4$ (sp)[d] | | 0.26 | 1.20 | --- | 18.6 | |
| | | 0.25 | 0.69 | --- | 28.2 | |

[a] Relative to $\alpha$-Fe.

[b] For magnetically split spectra this value is $2\varepsilon'$ ,$\Delta E_Q=2\varepsilon'$ if$\phi=0$.

[c] Ferrimagnetic $Fe_3O_4$.

[d] Superparamagnetic $Fe_3O_4$.

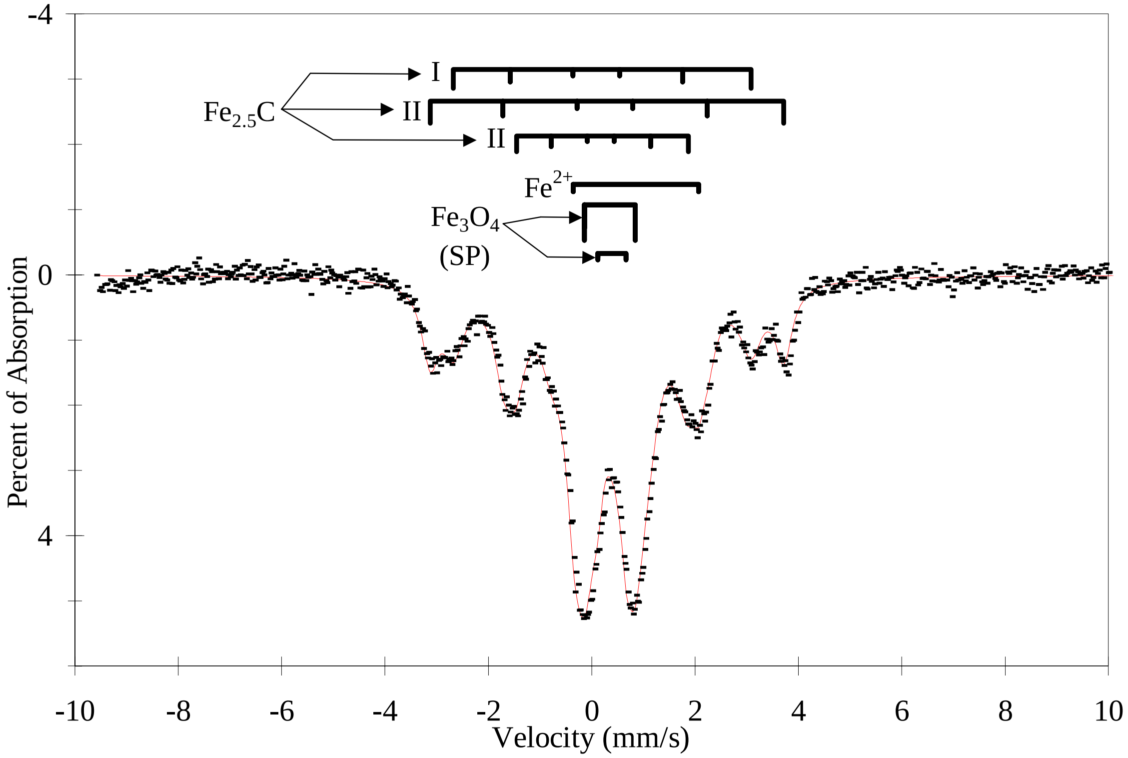

Fig 20. Mossbauer Spectrum of Fe-S-201 after statistically designed experiments run #08

SCA settings:
Window: 0.8 volts
Lower level: 5.6 volts
Course gain: 1 K
Fine gain: 0.532

Source to Counter distance: 7 inch
Count rate:16,809 counts/sec
Data collected at room temperature for 24 h

Table 17. Mössbauer spectroscopy parameters of Fe-S-201 catalyst after statistically designed fixed bed run # 08 at 265°C,10 atm, $H_2$/CO=1

| Species | Iron site | IS[a] mm/s | $\Delta E_Q$[b] mm/s | HFS KOe | % Area (298 K) | % Area (77 K) |
|---|---|---|---|---|---|---|
| <u>Fe-S-201 after 150 h</u><br><u>fixed bed test at 265°C P=1atm, $H_2$/CO=1</u><br>(spectra collected at 298K for 24 h) | | | | | | |
| $Fe_3O_4$ (FiM[c]) | | --- | --- | --- | --- | |
| | | --- | --- | --- | --- | |
| $\chi$-$Fe_{2.5}C$ | I | 0.15 | 0.11 | 178 | 19.4 | |
| | II | 0.28 | 0.04 | 212 | 17.1 | |
| | III | 0.19 | 0.03 | 103 | 12.9 | |
| $Fe^{2+}$ | | 0.86 | 2.42 | --- | 4.1 | |
| $Fe_3O_4$ (sp)[d] | | 0.35 | 0.98 | --- | 43.7 | |
| | | 0.39 | 0.55 | --- | 2.9 | |

[a] Relative to $\alpha$-Fe.

[b] For magnetically split spectra this value is $2\varepsilon'$ ,$\Delta E_Q = 2\varepsilon'$ if$\phi=0$.

[c] Ferrimagnetic $Fe_3O_4$.

[d] Superparamagnetic $Fe_3O_4$.

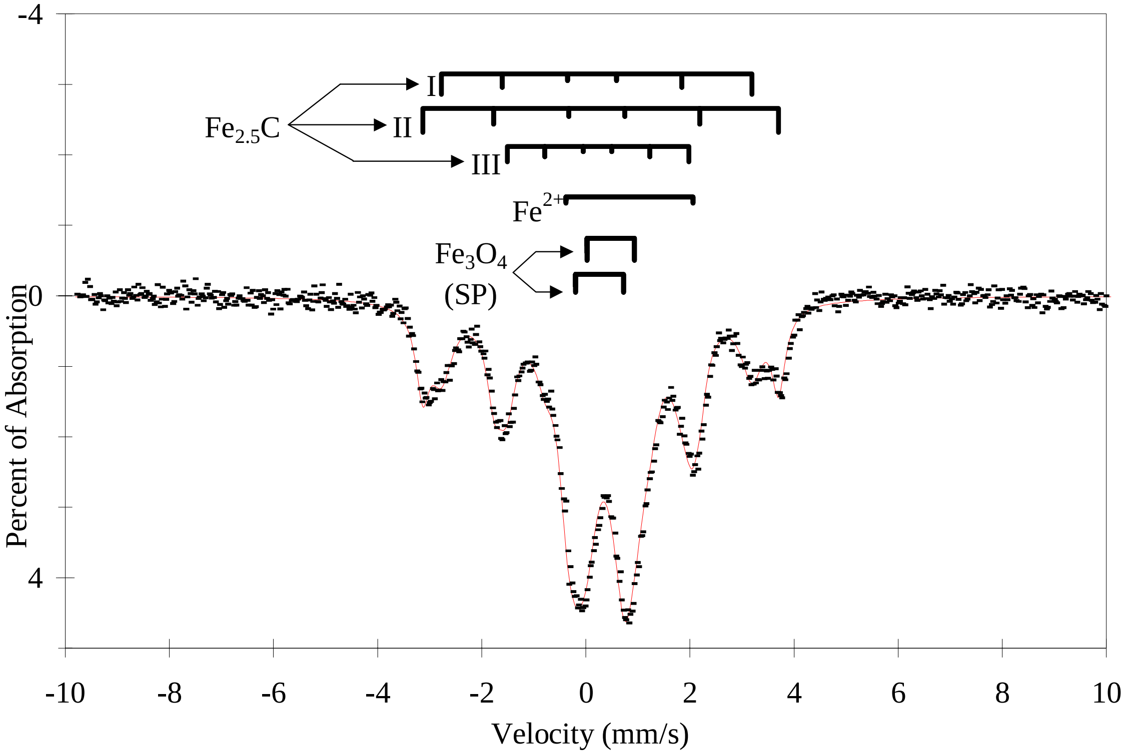

Fig 21. Mossbauer Spectrum of FePt-S-220 after statistically designed experiments run #09

SCA settings:
Window: 0.8 volts
Lower level: 5.6 volts
Course gain: 1 K
Fine gain: 0.532

Source to Counter distance:  7 inch
Count rate:15,640 counts/sec
Total Counts:1,348,976
Data collected at room temperature for 24 h

Table 18. Mössbauer spectroscopy parameters of FePt-S-220 catalyst after statistically designed fixed bed run # 09 at 265°C,10 atm, $H_2$/CO=1;Catalyst pretreated in $H_2$/CO=0.5, 320°C for 16 h

| Species | Iron site | IS[a] mm/s | $\Delta E_Q$[b] mm/s | HFS KOe | % Area (298 K) | % Area (77 K) |
|---|---|---|---|---|---|---|
| FePt-S-220 after 150 h<br>fixed bed test at 250°C P=1atm, $H_2$/CO=1<br>(spectra collected at 298K for 24 h) | | | | | | |
| $\chi$-$Fe_{2.5}C$ | I | 0.16 | 0.09 | 185 | 21.7 | |
| | II | 0.25 | 0.07 | 212 | 15.5 | |
| | III | 0.23 | 0.01 | 108 | 12.7 | |
| $Fe^{2+}$ | | 0.84 | 2.44 | --- | 3.6 | |
| $Fe_3O_4$ (sp)[c] | | 0.48 | 0.91 | --- | 28.5 | |
| | | 0.26 | 0.93 | --- | 17.9 | |

[a] Relative to $\alpha$-Fe.

[b] For magnetically split spectra this value is $2\varepsilon'$ ,$\Delta E_Q=2\varepsilon'$ if$\phi=0$.

[c] Superparamagnetic $Fe_3O_4$.

Table 19. Iron phases of unpromoted (Fe-S-201) and promoted (FePt-S-220, FePtK-S-218) catalysts after statistically designed fixed bed runs (room temperature Mössbauer)

| Catalyst | Run number | Iron species<br>% Area | | | |
|---|---|---|---|---|---|
| | | $Fe_3O_4$ (FiM)[a] | $Fe_{2.5}C$[b] | $Fe^{2+}$ | $Fe_3O_4$ (sp) |
| Fe-S-201 | 1 | 33.3 | 17.5 | 0.8 | 48.4 |
| Fe-S-201 | 2 | 2.2 | 41.4 | 5.3 | 51.2 |
| Fe-S-201 | 3 | 0.2 | 41.2 | 2.7 | 56.0 |
| FePt-S-220 | 4 | - | 41.1 | 5.8 | 53.0 |
| FePtK-S-218 | 5 | 4.0 | 31.8 | 4.8 | 59.4 |
| Fe-S-201 | 6 | 24.6 | 19.5 | 4.4 | 51.6 |
| FePtK-S-218 | 7 | 7.7 | 44.2 | 1.3 | 46.8 |
| Fe-S-201 | 8 | - | 49.4 | 4.1 | 46.6 |
| FePt-S-220 | 9 | - | 49.9 | 3.6 | 46.4 |

[a]:Ferrimagnetic $Fe_3O_4$

[b]:Haag or $\chi$-carbides ($Fe_{2.5}C$)

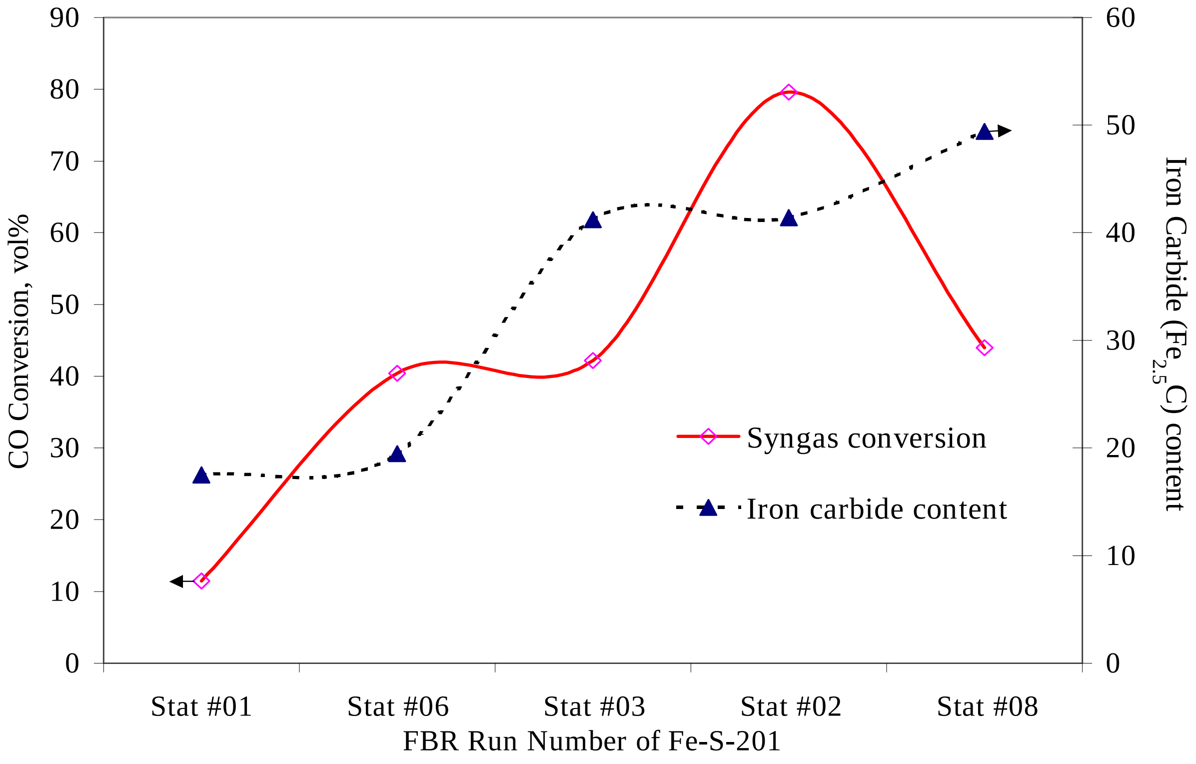

Fig 22. Syngas Conversion and Iron Carbide Content Correlation of Fe-S-201

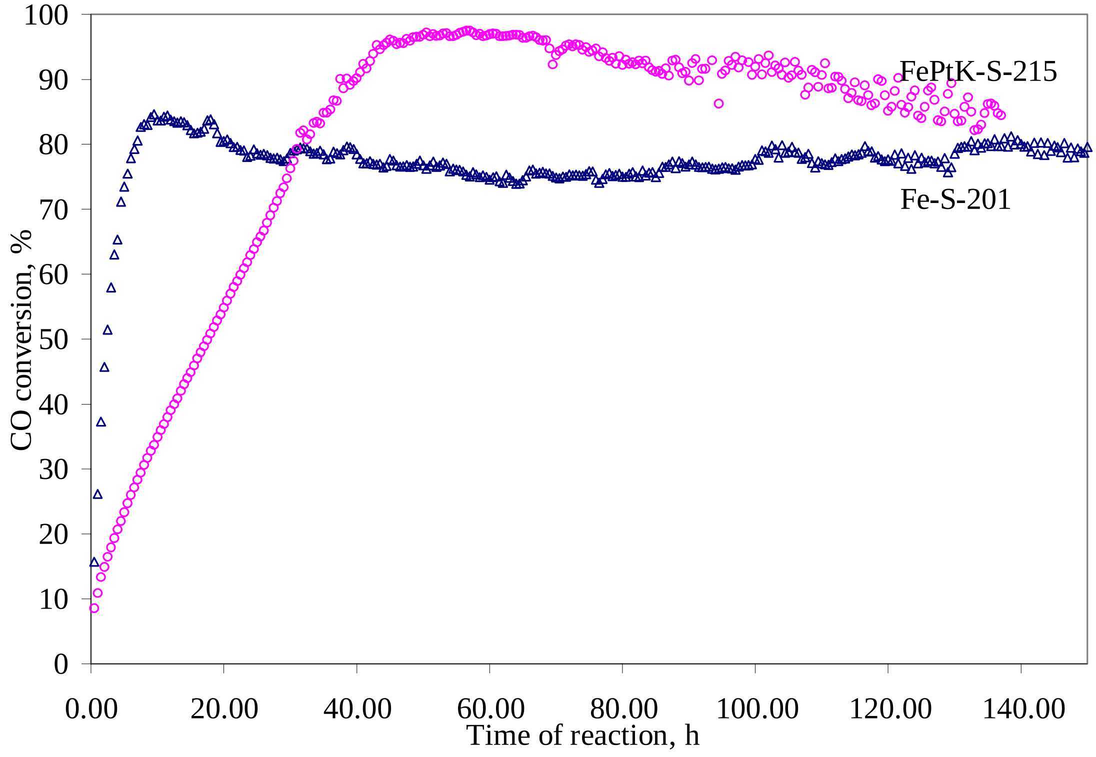

Fig 23. CO conversion of FePtK-S-215 compared with Fe-S-201 at 265°C, 10 atm,$H_2$/CO=1

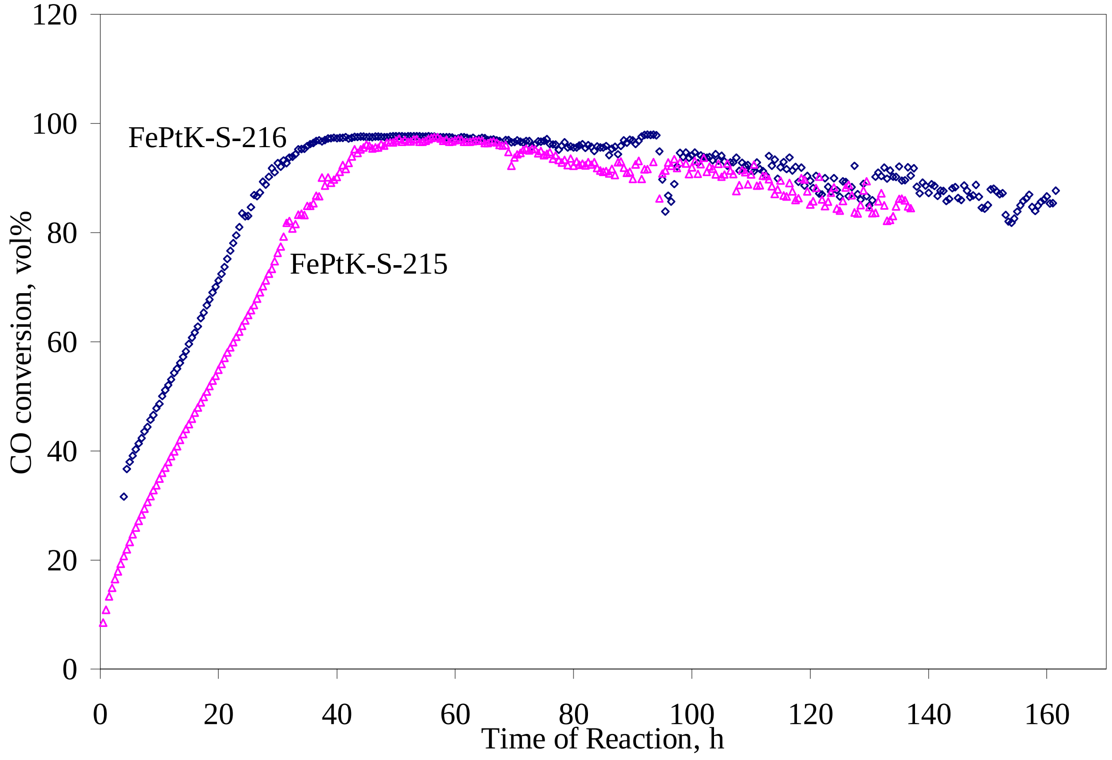

Fig 24. Repeatability of FePtK-S-215 and FePtK-S-216 fixed bed runs T=265°C,P=10 atm, Total Flow=64 sccm, $H_2$/CO=1

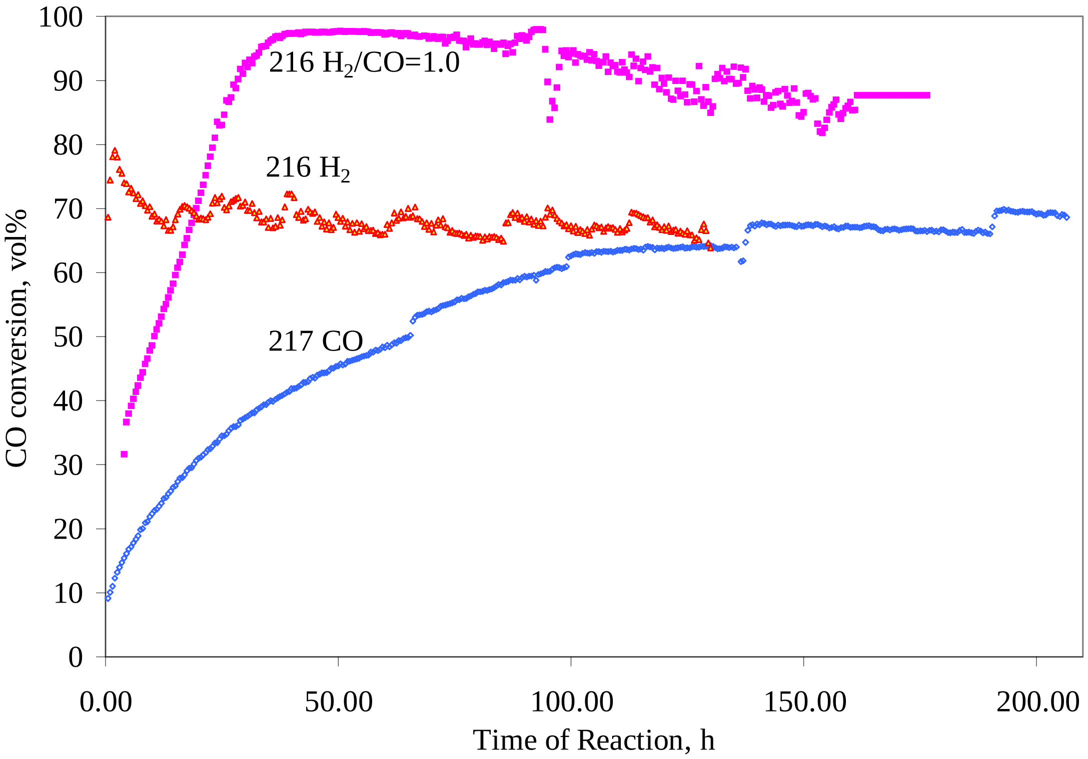

Fig 25. Pretreatment effects on FePtK-S-216 and FePtK-S-217

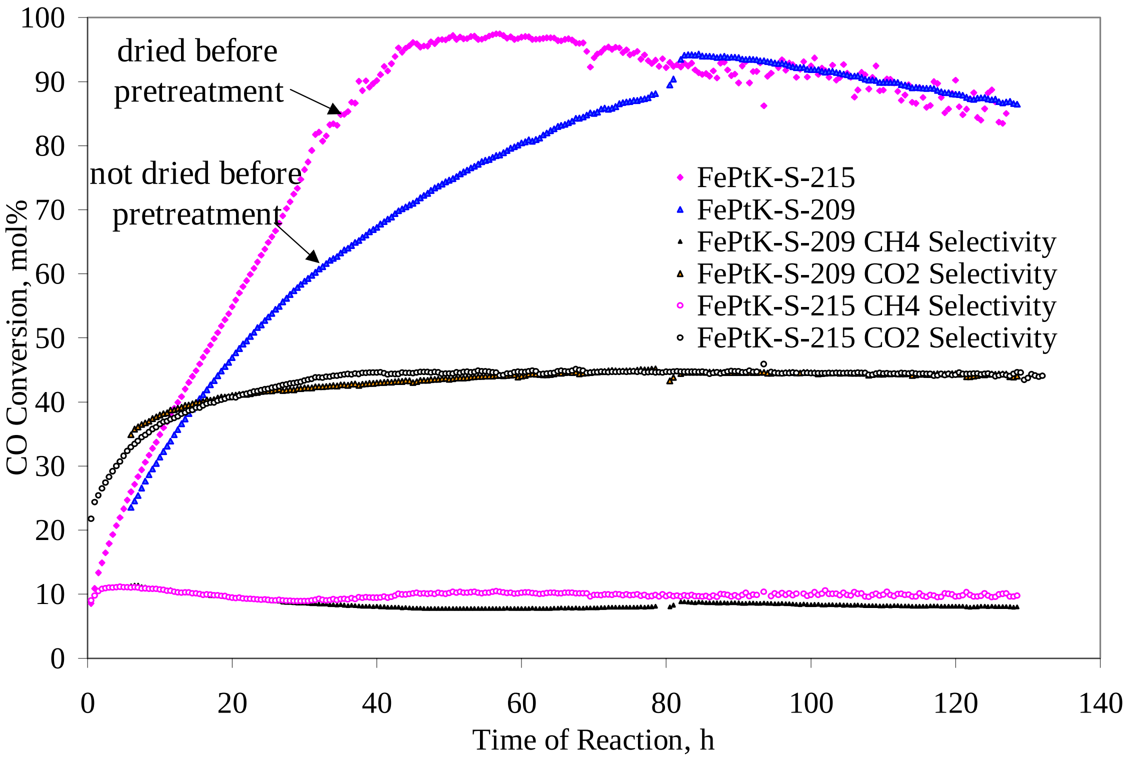

Fig 26. Fixed Bed Activity Comparision of FePtK-S-209 and FePtK-S-215

Table 20. Steady-state activity and selectivity for unpromoted (Fe-S-203, Fe-S-206) and promoted (FePt-S-203, FePt-S-206) catalysts[a].

| Catalyst | TOS (h) | Temp (°C) | Xco (%) | $-r_{CO}$x$10^6$ (mol/g-s) | ηk x $10^9$ (mol/g-s-$Pa^{0.5}$) | TOF ($s^{-1}$) | $S_{CH4}$ (%) | $S_{CO2}$ (%) |
|---|---|---|---|---|---|---|---|---|
| Fe-S-206[b] | 30 | 270 | 52.2 | 6.4 | 9.0 | 2.6 | 8.7 | 36.2 |
| | 35 | 270 | 51.1 | 6.3 | 8.8 | 2.6 | 8.7 | 35.6 |
| | 40 | 270 | 50.1 | 6.2 | 8.7 | 2.5 | 8.8 | 35.5 |
| | 49 | 270 | 48.5 | 6.0 | 8.4 | 2.4 | 8.9 | 34.9 |
| FePt-S-203[c] | 25 | 265 | 44.8 | 5.5 | 7.8 | 1.6 | 9.5 | 33.3 |
| | 35 | 265 | 43.4 | 5.3 | 7.5 | 1.6 | 9.5 | 32.8 |
| | 45 | 265 | 42.1 | 5.2 | 7.3 | 1.5 | 9.6 | 32.3 |
| | 61 | 265 | 40.3 | 5.0 | 7.0 | 1.5 | 9.7 | 31.9 |
| FePt-S-206[d] | 35 | 266 | 54.4 | 6.7 | 9.4 | 2.0 | 10.5 | 38.1 |
| | 45 | 265 | 58.0 | 7.1 | 10.0 | 2.1 | 10.2 | 38.7 |
| | 61 | 265 | 55.5 | 6.8 | 9.6 | 2.0 | 10.1 | 38.0 |
| | 140 | 265 | 57.1 | 7.0 | 9.9 | 2.1 | 10.7 | 38.8 |

[a] Catalyst loading: 2 g
Reaction conditions: 10 atm, $H_2$/CO=1, GHSV=1.92 NL/h/$g_{cat}$
PFR reactor assumed

[b] Fe-S-206 (10 wt% Fe); assume 6.8% dispersion; Davisil 644 supported

[c] FePt-S-206 (10 wt% Fe, 0.5 wt% Pt); assume 9.5% dispersion; Davisil 644 supported

[d] FePt-S-206 (10 wt% Fe, 1wt% Pt); assume 9.5% dispersion; Davisil 644 supported

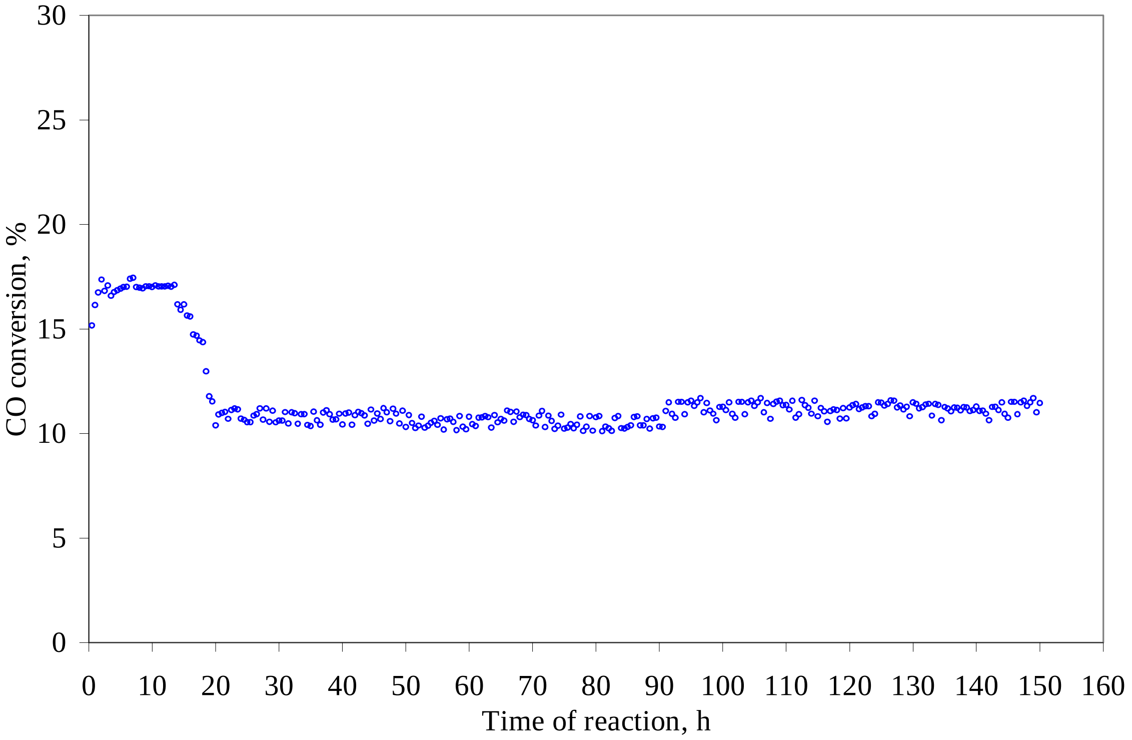

Fig 27. Statistically Designed Fixed Run 1 of Fe-S-201 Fixed Bed Run; Pretreated in $H_2$/CO=1,250°C, 16 h   Reaction conditions: T=250°C, P=10 atm, Total Flow=64 SCCM

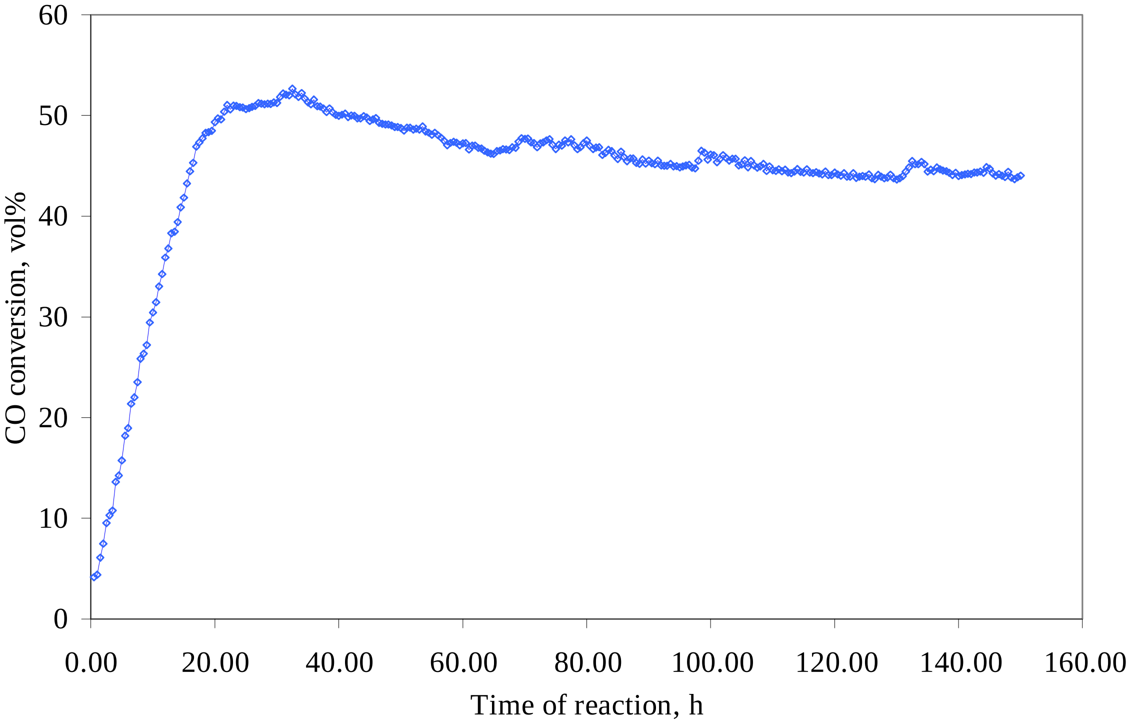

Fig 28. Statistically Designed Fixed Run 4 of FePt-S-220 Fixed Bed Run; Pretreated in $H_2$/CO=0.1,280°C, 16h   Reaction conditions: T=250°C, P=10 atm, Total Flow=64 SCCM

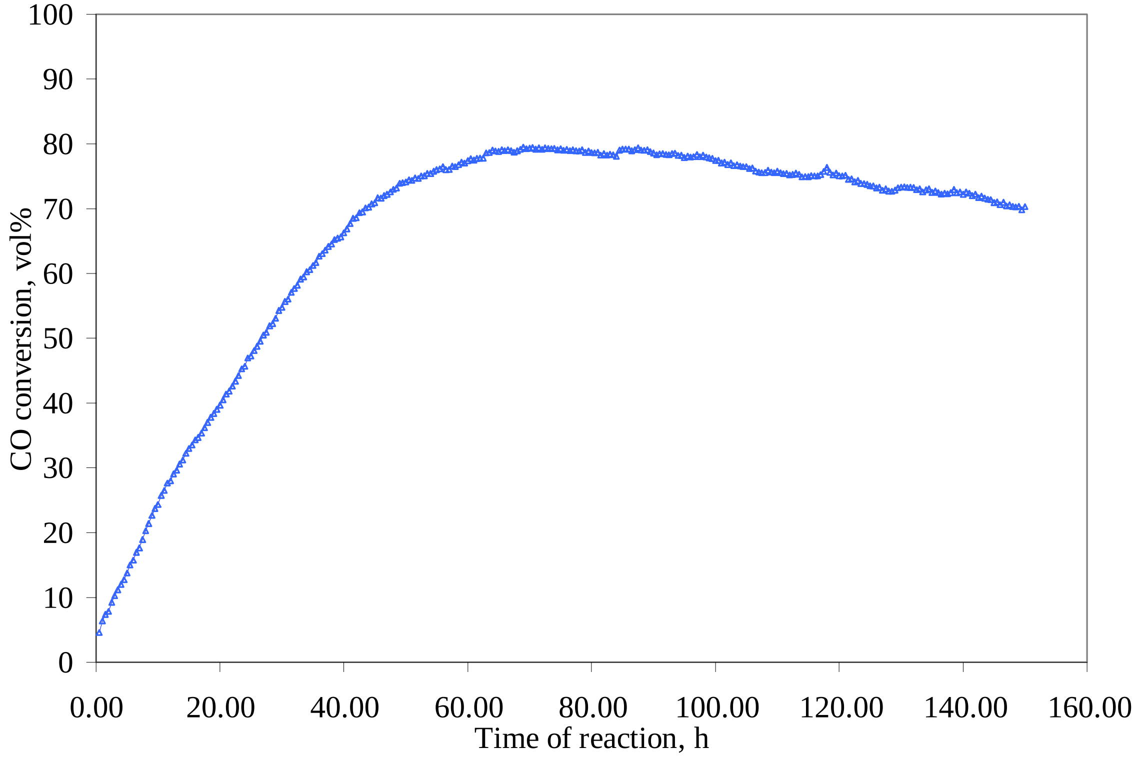

Fig 29. Statistically Designed Fixed Run 7 of FePtK-S-218 Fixed Bed Run; Pretreated in $H_2$/CO=1, 320°C, 16h Reaction conditions: T=265°C, P=10 atm, Total Flow=64 SCCM

Table 21. Steady-state activity and selectivity for unpromoted (Fe-S-201) and promoted (FePt-S-220, FePtK-S-218) catalysts[a] in statistically designed fixed bed runs

| Catalyst | Run number | TOS (h) | Reaction Temp (°C) | Xco (%) | $S_{CH4}$ (%) | $S_{CO2}$ (%) | Deactivation Rate (%/h)[b] |
|---|---|---|---|---|---|---|---|
| Fe-S-201 | 1 | 40 | 250 | 10.4 | 0.0 | 13.8 | |
| | | 150 | | 11.5 | 0.0 | 14.0 | 0.01 |
| Fe-S-201 | 2 | 40 | 265 | 78.5 | 12.7 | 49.5 | |
| | | 150 | | 79.6 | 12.5 | 50.1 | 0.01 |
| Fe-S-201 | 3 | 40 | 250 | 45.4 | 8.3 | 34.3 | |
| | | 150 | | 42.2 | 8.6 | 32.8 | -0.029 |
| FePt-S-220 | 4 | 40 | 250 | 45.0 | 8.9 | 37.2 | |
| | | 150 | | 44.0 | 7.4 | 33.3 | -0.009 |
| FePtK-S-218 | 5 | 40 | 265 | 74.4 | 10.6 | 52.1 | |
| | | 150 | | 74.9 | 8.7 | 49.9 | 0.0046 |
| Fe-S-201 | 6 | 40 | 265 | 40.6 | 9.6 | 33.4 | |
| | | 150 | | 40.4 | 8.7 | 33.4 | -0.0018 |
| FePtK-S-218 | 7 | 40 | 250 | 66.3 | 9.8 | 49.5 | |
| | | 150 | | 70.3 | 7.0 | 47.5 | 0.036 |
| Fe-S-201 | 8 | 40 | 250 | 31.4 | 9.5 | 25.6 | |
| | | 150 | | 44.0 | 8.8 | 33.2 | 0.115 |

[a] Catalyst loading: 2 g
Reaction conditions: 10 atm, $H_2$/CO=1, GHSV=1.92 NL/h/$g_{cat}$
PFR reactor assumed
[b] Assume linear deactivation